

Study of Bauschinger Effect in Various Spring Steels

by

Jun Yan

**A thesis submitted in conformity with the requirements
for the degree of Master of Applied Science
Graduate Department of Metallurgy & Materials Science
University of Toronto**

© Copyright by Jun Yan 1998



**National Library
of Canada**

**Acquisitions and
Bibliographic Services**

**395 Wellington Street
Ottawa ON K1A 0N4
Canada**

**Bibliothèque nationale
du Canada**

**Acquisitions et
services bibliographiques**

**395, rue Wellington
Ottawa ON K1A 0N4
Canada**

Your file Votre référence

Our file Notre référence

The author has granted a non-exclusive licence allowing the National Library of Canada to reproduce, loan, distribute or sell copies of this thesis in microform, paper or electronic formats.

The author retains ownership of the copyright in this thesis. Neither the thesis nor substantial extracts from it may be printed or otherwise reproduced without the author's permission.

L'auteur a accordé une licence non exclusive permettant à la Bibliothèque nationale du Canada de reproduire, prêter, distribuer ou vendre des copies de cette thèse sous la forme de microfiche/film, de reproduction sur papier ou sur format électronique.

L'auteur conserve la propriété du droit d'auteur qui protège cette thèse. Ni la thèse ni des extraits substantiels de celle-ci ne doivent être imprimés ou autrement reproduits sans son autorisation.

0-612-45601-3


Study of Bauschinger Effect in Various Spring Steels

By Jun Yan

Degree of Master of Applied Science, 1999
Department of Metallurgy and Materials Science
University of Toronto

Abstract

It is recognized that the effective life of automotive suspension springs could be ended by yielding rather than fracture. The industry describes this problem as load loss or sag. Recent trends to design and manufacture light-weight automobiles result in higher working stress in springs requiring a further improved sag resistance of spring steels. The present study is conducted to characterize the sag behavior of the SAE 5160H, 9259V, and Duraspring steels by using Bauschinger effect test. Results of this systematic study showed that 9259V demonstrated a stronger Bauschinger effect compared to 5160H and Duraspring steels. Consequently, 9259V should have a better sag resistance over all. The effects of hardness level on Bauschinger effect were also established. The magnitude of Bauschinger effect reached a peak value when 9259V was hardened to HRc 50 and tested with 1% of pre-plastic strain. However, for 5160H and Duraspring steels, only a continuous reduction in Bauschinger effect with increasing in hardness has been observed. Silicon was realized to be the major alloy element influencing Bauschinger effect. The greater the silicon content in the steel, the larger the Bauschinger effect, and therefore, the better the sag resistance of the spring. In addition to silicon, carbon content also plays a role to affect Bauschinger effect. The results from present study can provide the basis for both the design of new spring steels and the modification of the existing spring steels.



The author wish to acknowledge his grateful thanks to his supervisor Professor Zhirui Wang for his ever-available guidance, most knowledgeable and valuable advice, encouragement, and confidence through out the entire course work and research. The author is also like to thank Dr. Z.A. Yang, Dr. G. Bo, Dr. T.K. Yip, Dr. S. Sun, Ms. R. Zhang, and Mr. H. Ni for their invaluable discussions, comments and generous help on this project. The author would also like to express his appreciation to Mr. J. Calloway and Mr. F. Neub for their kindly support. Finally, the author would like to thank STELCO Ltd., Inland Steel Ltd. for their generous support and making this project possible.

| | |
|-----------------------------------------|------------|
| Abstract | I |
| Acknowledgements | II |
| Table of Contents | III |
| List of Figures and Tables | VI |

Chapter 1

Introduction

| | | |
|-------|------------------------------------------------------------------|----|
| 1.1 | Automobile suspension spring and steels..... | 1 |
| 1.2 | Main factors in spring design..... | 3 |
| 1.3 | Sag behavior..... | 4 |
| 1.4 | Bauschinger effect and its mechanisms..... | 7 |
| 1.4.1 | Bauschinger effect..... | 7 |
| 1.4.2 | Mechanisms of Bauschinger effect..... | 10 |
| 1.4.3 | Evaluation of the magnitude of Bauschinger effect..... | 16 |
| 1.5 | Effect of silicon on tempering of spring steels..... | 24 |
| 1.5.1 | The significance of silicon content in the spring steels..... | 24 |
| 1.5.2 | Tempering of steels..... | 25 |
| 1.5.3 | Effect of silicon content on the tempering of spring steels..... | 27 |
| 1.6 | Objectives..... | 30 |
| 1.7 | Reference..... | 31 |

Chapter 2

Experimental setup and procedures

| | | |
|-------|-----------------------------------------------|----|
| 2.1 | Materials..... | 34 |
| 2.2 | Test sample preparation..... | 35 |
| 2.2.1 | Test specimen..... | 35 |
| 2.2.2 | Heat treatment..... | 36 |
| 2.2.3 | Microstructure..... | 39 |
| 2.3 | Mechanical testing..... | 39 |
| 2.3.1 | Hardness test..... | 39 |
| 2.3.2 | Material testing system..... | 40 |
| 2.3.3 | MTS setup and procedures..... | 40 |
| 2.3.4 | Tensile test and Bauschinger effect test..... | 41 |
| 2.4 | Reference..... | 43 |

Chapter 3

Results

| | | |
|-----|-------------------------------------------------------------|----|
| 3.1 | Tempering behavior..... | 44 |
| 3.2 | Mechanical properties..... | 46 |
| 3.3 | Microstructures..... | 50 |
| 3.4 | Bauschinger effect test..... | 55 |
| 3.5 | Examination of silicon and inclusions in spring steels..... | 61 |

Chapter 4

Discussions

| | | |
|-------|---------------------------------------------------------------|----|
| 4.1 | Effect of silicon on tempering behavior of spring steels..... | 63 |
| 4.1.1 | Effect on hardness..... | 63 |
| 4.1.2 | Effect on microstructures..... | 70 |
| 4.2 | Bauschinger effect..... | 71 |
| 4.2.1 | Bauschinger effect Vs pre-plastic strain..... | 71 |
| 4.2.2 | Bauschinger effect Vs hardness..... | 75 |
| 4.3 | Estimation for weight saving..... | 78 |
| 4.4 | Reference..... | 81 |

Chapter 5

| | |
|-------------------------|-----------|
| Conclusions..... | 83 |
| Future work..... | 85 |

- Figure 1.1** Schematic representation of Loop Area and ABT in Bauschinger torsion test.
- Figure 1.2** Schematic representation of the uniaxial stress-strain behavior of many materials during forward and reverse flow tests showing Bauschinger effect.
- Figure 1.3** Schematic representation of the composite model using materials with the same Young's modulus and hardening behavior but different yield strengths.
- Figure 1.4** Schematic representation of a dislocation pileup and a mobile dislocation line interact with several sessile point dislocations.
- Figure 2.1** Specimen dimensions for all the tension and Bauschinger effect tests (all dimensions in mm).
- Figure 2.2** Heat treatment cycles for 5160H, 9259V, and Duraspring steels.
- Figure 3.1** Hardness vs tempering temperature curves for 5160H, 9259V, and Duraspring steels.
- Figure 3.2** Stress – strain curves for Microstructures 5160H, 9259V, and Duraspring steels tempered to HRc 48 and tested at room temperature. of 5160H, 9259V, and Duraspring steels tempered at 500 °C for 1h, 2% nital ecth, 800×.
- Figure 3.3** Microstructures of 5160H, 9259V, and Duraspring steels quenched at 905 °C for 1h, 2% nital ecth, 800×.
- Figure 3.4** Microstructures of 5160H, 9259V, and Duraspring steels tempered at 250 °C for 1h, 2% nital ecth, 800×.
- Figure 3.5** Microstructures of 5160H, 9259V, and Duraspring steels tempered at 350 °C for 1h, 2% nital ecth, 800×.

- Figure 3.6** Microstructures of 5160H, 9259V, and Duraspring steels tempered at 450 °C for 1h, 2% nital ecth, 800×.
- Figure 3.7** Microstructures of 5160H, 9259V, and Duraspring steels tempered at 550 °C for 1h, 2% nital ecth, 800×.
- Figure 3.8** Schematic representation of room temperature Bauschinger effect tests for Duraspring steel tempered to HRc 48 at different pre-plastic strain levels.
- Figure 3.9** Bauschinger stress parameter vs pre-plastic strain for 5160H, 9259V, and Duraspring steels tempered to HRc 47.5.
- Figure 3.10** Bauschinger stress parameter vs. hardness curves for 5160H, 9259V, and Duraspring steels at 1 % pre-plastic strain.
- Figure 3.11** Bauschinger stress parameter at 1% pre-plastic strain vs. the total content of carbon and 1/3 of silicon among 5160H, 9259V, and Duraspring steels.
- Figure 3.12** X-ray mapping analysis of silicon and image of MnS inclusion in 9259V.
- Figure 4.1** Martensite body – centered tetragonal lattice illustrating the three sets of octahedral intersites.
- Figure 4.2** The nature of the sites that interstitial carbon atoms occupy in the body – centered cubic iron lattices.
- Figure 4.3** Effect of several elements on the hardness of martensite tempered in temperature range from 205 °C to 705 °C for 1h.
- Figure 4.4** Effect of several elements on the hardness of martensite tempered in temperature range from 205 °C to 705 °C for 1h.
- Table 2.1** Chemical Composition of the Steels Investigated, wt.%.
- Table 3.1** As quenched hardness of 5160H, 9259V, and Duraspring steels.

Table 3.2 Mechanical properties of 5160H, 9259V, and Duraspring steels.

Table 4.1 Estimation of weight saving of suspension springs.

Table 4.2 Calculation of weight saving of suspension springs.

Chapter 1

1.1 Automobile suspension spring and steels

The main function of automotive suspension springs is to provide smooth and even ride. Therefore, the ability to withstand the weight of an automobile without incurring appreciable setting or relaxation is an important performance characteristic of automobile suspension springs. During service, springs are subjected to fatigue loading which is normally lower than the yield strength of the spring material. However, the design and mount is such that yielding anywhere in the spring is prevented. Moreover, the springs are given a preload before being mounted on the vehicle. This process called scragging or presetting, in addition to strain hardening, gives the necessary plastic accommodation. Nevertheless, with service time, springs progressively deform or sag. Although nominal relaxation of springs is expected and usually poses no serious problem, there are several practical reasons why the relaxation characteristics of springs deserve serious consideration: (1) Unusually excessive relaxation of the front - coil springs of an automobile, and the attendant settling of the front - end, might interfere with the driver's ability to steer the car safely. (2) Both Canadian and US Federal Governments have issued safety - motivated regulations that stipulate the limits for the bumper heights of new automobiles. (3) Spring relaxation is one of the factors that must be taken into account in design changes to improve riding quality. It is functionally practicable to have the lowest spring rate (the ratio of spring height H and main coil diameter D) or stiffness for a good ride. However, a lower spring rate is usually associated with lower relaxation resistance and, therefore, it is necessary to use a steel that can provide a good sag

resistance for desired spring rate. (4) As part of the recent trend towards smaller, lighter - weight automobiles, the weight reduction of suspension springs has been awaited with great interest. However, any weight reduction will also result in a higher stress level on the springs. Such a higher stress level inevitably presents the problems of increased sagging of the springs. In view of the foregoing, springs must have good surface quality, hardenability; especially sag resistance to meet the applications. These requirements clearly demanded the development of spring steels, which possess high sag resistance, even under severe stress condition. In order to improve sag resistance, raising the hardness or the strength of spring steel from which the springs are made is one of the simplest and most effective ways to do it. However, if the fatigue strength is reduced by raising the hardness, the springs will not be suitable for the applications. To prevent this problem, it is necessary to raise the hardness by strengthening the matrix of the material only to the extent that it does not cause a reduction of the fatigue life. Traditionally, automobile suspension springs are manufactured out of hot - rolled alloy bars. The significant features of the manufacturing processes are heating to the austenitizing temperature, hot coiling, oil quenching, tempering to desired hardness level, shot peening, and cold setting. In addition to this conventional way, there are several other methods of strengthening the matrix of spring steels.

- 1) **Increase Silicon content:** In this method, the content of Si, a ferrite matrix strengthener, is increased and this results in solution and theta carbide dispersion strengthening during tempering. This method has been used commercially in Si - Mn steels (SAE 9260).
- 2) **Add V, Cb, and Mo:** The elements V, Cb, and Mo are carbide formers in steel and promote precipitation hardening. The refining of crystal grains is a by - product of this addition.

3) **Refining of crystal grains:** The yield point is increased by refining crystal grains. Grain refinement can also be accomplished by thermal treatment. Rapid induction heating and quenching after holding the material for a short period of time in the austenite zone is an exceedingly effective way of thermal treatment ^[1.1].

Over the years, a number of alloys have been used for hot - formed springs. Chromium - containing AISI 5160 (0.70-0.90 pct Cr) and modified 5160 (0.45-0.65 pct Cr.) are at the top of the list in terms of wide use, followed by three other alloy steels and carbon steels. Except for AISI 1095 and AISI 6150, the maximum carbon for these spring steels is about 0.65 pct, which is apparently considered the safe upper limit for spring steels with good hardenability. Higher carbon will increase the danger of quench cracking for those bars small enough to through - harden. AISI 9260, Silicon - containing (1.8 - 2.2% Si) has been commonly used for automotive springs for many years. AISI 9260 was recommended for use in highly stressed applications. Actually, steels with high silicon content, as in the case of AISI 9260, have a reputation for excellent load - loss resistance or sag resistance among conventional steels, but because of its high silicon content this steel may have relative poor surface quality, i.e., it is easily decarburized, which leads to poor fatigue life. In the present project, we selected the spring steels that have been widely used or newly developed to study their sag behaviors at different hardness or strength levels. They are 5160H, 9259V and Duraspring steels respectively. The chemical compositions of these three steels are listed in the table 2.1.

1.2 Main factors in spring design

Speaking of spring design, there are some main factors have to be concerned. First is the strength of the material. In automotive industry, it has been recognized that the effective life

of automotive springs is usually ended by yielding rather than fracture, therefore, the elastic limit has a direct influence on spring properties. In general, the criterion σ_f^2/E is used for material selection and manufacturing, where σ_f is the stress to fracture and E is Young's modulus. It is commonly accepted that the higher the value of this expression, the better the material is for making mechanical springs. Second is the fatigue strength. Suspension springs are made for lifetime service, therefore, a high endurance limit is desired. Third is sag resistance. As springs progressively deform or sag with service time, the ability to withstand the weight of an automobile without incurring relaxation becomes an important character. In addition, weight reduction is also an inevitable factor for spring design because any weight saving would result in higher working stresses that can be high fraction of the yield stress of the material. Although all of these factors have to be taken into serious consideration during the spring design, the present project is mainly focused on the study of sag behavior of automotive springs by using Bauschinger effect test. Bauschinger effect itself is the weakening phenomenon of material when it is deformed in the reverse direction after a plastic strain in a forward direction. It serves to predict the potential sag resistance of spring steels. The greater the Bauschinger effect of the spring steel, the better the sag resistance of the material.

1.3 Sag behavior

Springs, such as automobile suspension springs, would experience a decrease in the length or the height during service as time has gone by. It has been recognized by industry as sag or relaxation. Sag is a relaxation phenomenon that results in a reduced load carrying capability. It may result from both static and dynamic loading during service and is

logarithmically dependent on time. More precisely, sag is the phenomenon whereby a cyclic microcreep and/or plastic deformation, mainly cyclic softening, have occurred over a large number of loading cycles at nominal stress levels clearly below the material's yield strength. A cyclic microcreep mechanism, therefore, could be responsible for the overall relaxation of the spring by its cumulative effect over several thousand loading cycles. The spring operating stresses may introduce microplastic deformation at stress levels, which are nominally in elastic region, and the extent of such yielding could be different from steel to steel. Sag resistance is best measured by direct static and dynamic tests on prototype springs. In static test, sag resistance is measured by means of load loss at some fixed spring deflection after a sustained loading at some predetermined level for a predetermined time (a few days). In dynamic test, the load loss is measured after a fatigue loading between predetermined limits for a predetermined number of cycles. However, a direct evaluation of sag resistance has the following disadvantages. First, it is very time consuming to performing load loss experiments. Even for a simple static test, it could take up to a few months. Second, expensive coil making facilities must be available to make the test specimens as well as special fatigue test machine has to be available to perform the dynamic test. Furthermore, the amount of steel required is sizable because anywhere from 10 to 15 feet of spring steel bar goes into typical springs intended for automotive use. Moreover, the surface qualities, geometrical inhomogenities, etc. of springs are bound to affect the sag properties in addition to the properties of the spring steel itself. Furr^[1,2] proposed the Bauschinger torsion test as a convenient method to avoid such requirements associated with load loss test. He suggested that the static load-loss test is really a kind of torsional stress-relaxation test, since stress relaxation is defined as a decrease in stress at a constant deformation. When a coil spring is

deflected by axial loading, the spring bar is twisted in torsion. In fact, the spring can be considered a long torsion bar with a length proportional to the product of the mean coil diameter and the number of active coils in the springs. Thus, the static load-loss test of coil springs is a torsional stress-relaxation test of a very long torsion bar, assuming that the axially loaded coil spring behaves like a straight bar in pure torsion. The conventional torsion test reveals the torque-twist diagram, which is a measure of the stress-strain curve of the material in one direction of twist only. The Bauschinger torsion test, see Fig.1.1, measures the weakening of metal when it is strained in the reverse direction after a plastic strain in a forward direction, by using the "Actual Bauschinger Twist"(ABT) which measures the difference in strain between the forward-twist and reverse-twist curve at maximum torque. Torsional Bauschinger tests showed that the better spring steel, AISI 9260, has a larger Bauschinger effect than 5160 steel. Since springs are energy-storage devices, the better spring steels must have considerable resilience. Resilience is the ability of a material to recover its original size and shape after deformation caused by stress. Thus, the results conclude the correlation that the larger Bauschinger effect means better resilience. Since the Bauschinger effect is correlated with the parameters associated with the resilience and with the known ratings of resistance to sag or load loss, the Bauschinger effect can be served as a test to predict the relative sag or load loss resistance of spring steels. Although the Bauschinger effect test can be employed as a rapid technique to predict the potential load lose or sag resistance of spring steels, the mechanisms of Bauschinger effect are not the cause of sag because the former occurs only on the first few cycles of loading and the latter occurs over thousands of cycles at stresses which are normally elastic.

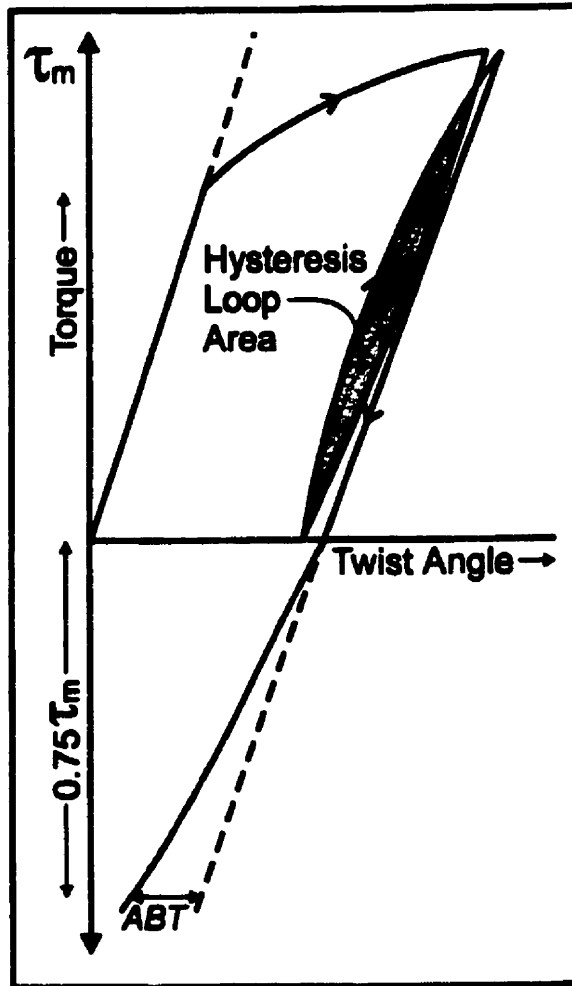


Fig 1.1 Schematic representation of Loop Area and ABT in Bauschinger torsion test^[1.3].

1.4 Bauschinger effect and its mechanisms

1.4.1 Bauschinger effect

When materials are loaded uniaxially in one direction (e.g. in tension) into the plastic regime, unloaded to zero stress level, then reloaded in reverse direction (e.g. in compression), they may yield during the reloading, at a stress level lower than if the reloading were carried out in the original direction. Figure. 1.2 is the schematic representation of Bauschinger effect test.

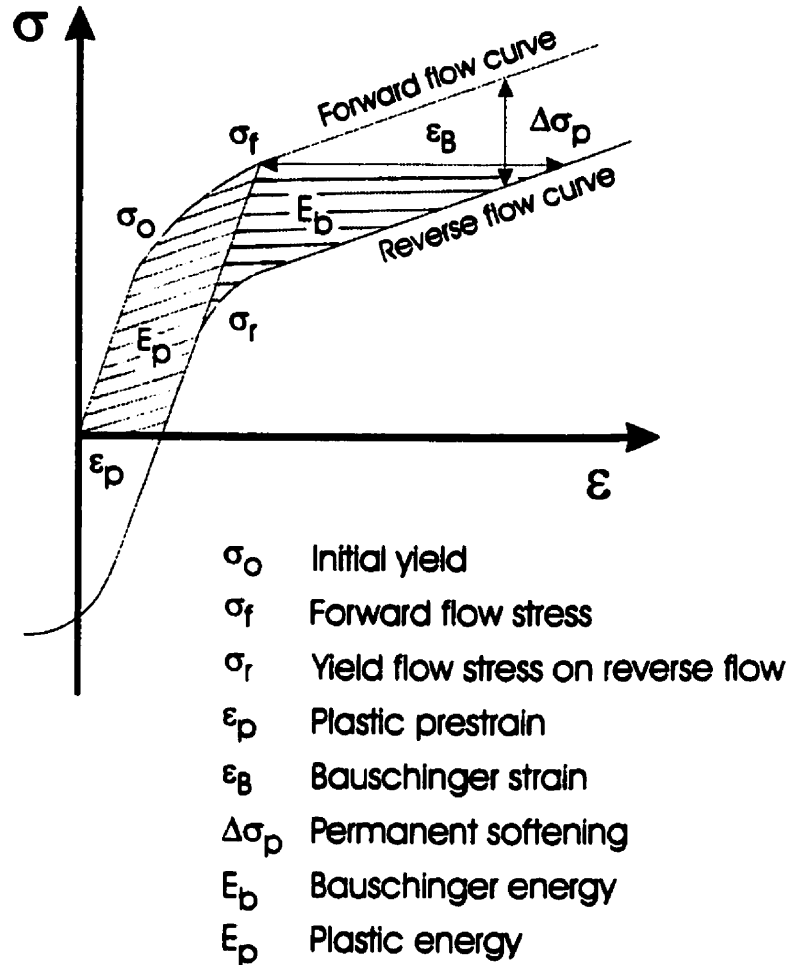


Fig 1.2 Schematic representation of the uniaxial stress-strain behavior of many materials during forward and reverse flow tests showing Bauschinger effect^[1.4].

This direction-dependent, asymmetrical yield behavior is known as the Bauschinger effect, after Johann Bauschinger^[1.5] who first reported this phenomenon in 1886. This effect has been widely studied since then. It is now clear that Bauschinger's discoveries dealt with only a part of the phenomena involved and that directional behavior in the stress-strain relationship is more complex than original thought. In view of these complexities it is not

surprising that many different features have been used in describing the Bauschinger effect.

For example:

‘ If a specimen is highly deformed in one direction and then immediately reloaded in the opposite direction, it began to flow in this direction at a reduced stress. This is the Bauschinger effect.’ Cottrell^[1.6].

‘ The Bauschinger effect is measured by the Bauschinger strain β .’ Buckley and Entwistle^[1.7].

‘ Originally observed in polycrystals, but later found to be present also in single crystal, the Bauschinger effect denotes a certain dependence of the flow stress and rate of work hardening on the strain history of the metal.’ Van Bueren^[1.8].

‘ The lowering of yield stress when deformation in one direction is followed by deformation in opposite direction is called the Bauschinger effect.’ Dieter^[1.9].

‘ The Bauschinger effect involved not only a premature yielding, but also a certain amount of permanent softening or non strain hardening strain.’ McClintock and Argon^[1.10].

These definitions above represent many different features of the Bauschinger effect. The main characteristics of the Bauschinger effect as normally understood are shown in Fig. 1.2. In order to have a convenient comparison, the stress forward and in reverse deformation are plotted in the same direction and against plastic prestrain. Since J. Bauschinger’s discovery, the Bauschinger effect has been shown to occur in a variety of materials: from single crystal to polycrystals, from pure metal to alloys, to dispersion hardened metals. Wolley^[1.11] observed that the Bauschinger effect was more pronounced in fcc materials compared to the bcc materials. Moreover, in recent years, the study in MMC has provided a good way in understanding deformation in these materials. In essence, the Bauschinger effect reflects a material deviation from ideal plastic behavior.

1.4.2. Mechanisms of the Bauschinger effect

Many studies have been carried out to explain the Bauschinger effect since the discovery of this effect. Early ideas about the cause of the Bauschinger effect were believed to be the internal stresses, and macroscopic residual stresses developed due to non-homogeneous deformation of individual grains of a polycrystalline metal. Orowan's^[1.12] ideas, on the other hand, suggested an alternative explanation based on anisotropy of the driving force for dislocation motion, due to prestrain. In general, there are two main schools advanced to explain the Bauschinger effect, internal stress and dislocation theories. In addition, the Bauschinger effect can be described by a composite model, which was first proposed by Masing.

1) Internal stress theory

Heyn (1918) developed a theory to explain the yield stress lowering observed at load reversal. Three assumptions were made by Heyn^[1.13]:

- (1) The material consists of small volume elements, which have ideal stress-strain curve: the elastic response changes into a non-hardening plastic extension at a constant stress level.
- (2) The elastic limits of various volume elements are not equal to each other.
- (3) The absolute value of elastic limit of any volume element is independent of the direction of deformation, that is the same in tension and in compression.

With these assumptions, the theory explains that: there is a curvature in the initial stress-strain curve at the elastic-plastic transition. During deformation, strain is homogeneously uniform in the load section. During plastic deformation, the stress distribution is not uniform; therefore, after unloading, residual stresses arise which are responsible for the yield-lowering

effect upon load reverse. These ideals were strongly supported by tension-compression test carried out by Masing^[1.14] on brass, and the results of torsion test on iron, brass, copper, and aluminum wires. The Bauschinger effect was explained as being due to the action of internal stresses locked up in cold worked metal by Schmid and Boas^[1.15].

2) Composite model

The Bauschinger effect also can be described by a composite model, see Fig.1.3, whenever two phases (matrix and second phase, etc.), or two components, with different mechanical properties exist in a single specimen. This model was first proposed by Masing. The model suggested that there are two phases or two components in a specimen, they have the same elastic constant, but different elastic limits.

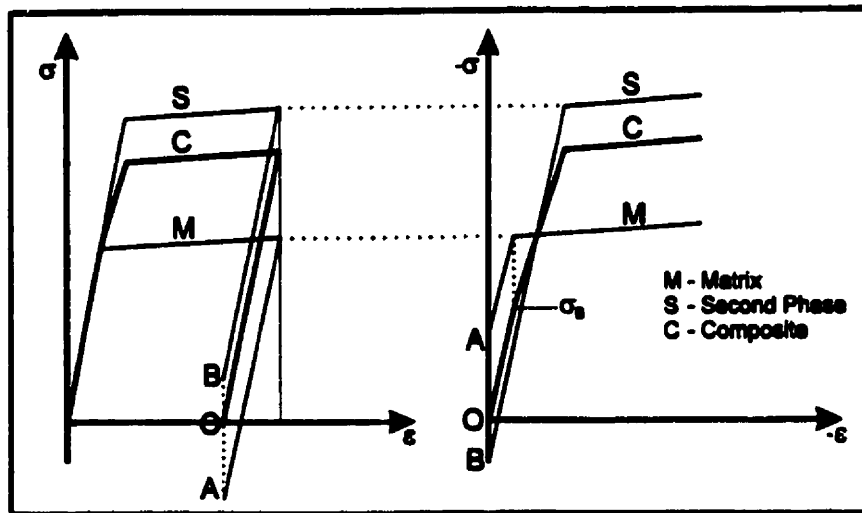


Fig. 1.3. Schematic representation of the composite model using materials with the same Young's modulus and hardening behavior but different yield strengths ^[1.16].

When the specimen undergoes the same prestrain in one direction, if this strain is sufficiently high, plastic deformation will occur in the phase or component which has the

lower elastic limit, while the other one will behave elastically. On unloading, when the applied load is zero, one phase or component will be in tensile stress and the other one will be in compressive residual stress. On reloading in the same direction, to the same stress level, both will behave elastically; but on reloading in the opposite direction, the residual stress in the 'softer' phase or component will help the applied stress to cause premature yield. Thus the behavior is asymmetrical and the system is softer for the reverse loading than it was in virgin state. Masing's model also occurs in materials where Young's modulus and the hardening behavior are different in the matrix and second phase.

3) Dislocation theory

Internal stress theory is greatly weakened when one takes account of the results of numerous experiments which have demonstrated the existence for a Bauschinger effect in single crystals, therefore, a different approach is needed for the explanation of the Bauschinger effect. There are two main dislocation approaches: The first one was originally given by Mott^[1.17] and later developed by Seeger^[1.18]. It was suggested that during prestraining a long range stress is built up through the formation of dislocation pile-up at barriers. Fig.1.4 demonstrates dislocations piled up at obstacles that defined as barriers.

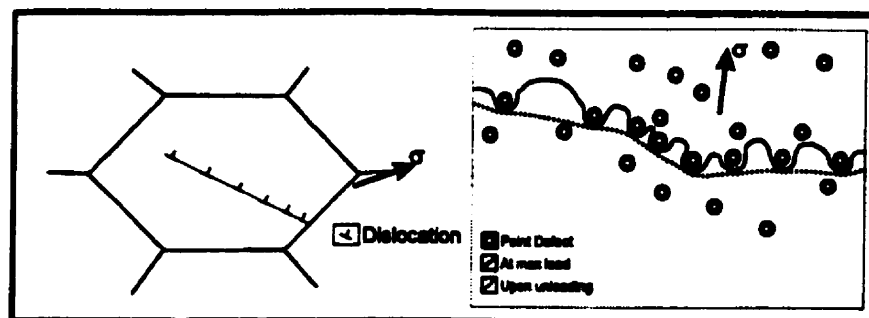


Fig 1.4 Schematic representation of a dislocation pileup and a mobile dislocation line interacting with several sessile point dislocations^[1.19].

These barriers, such as grain boundaries, are strong enough to block the motion of dislocations. As a result, the back stresses produced by dislocation piled up will assist motion in the reverse direction. Thus, the equation for flow stress can be described as follows:

$$\tau_i = \tau_F + \tau_{BK} \quad (1.1)$$

Where τ_{BK} is the back stress developed by dislocation piled up; τ_F is the frictional stress on the glide plane; and τ_i is the applied stress. The above equation indicates that the larger the τ_{BK} , the lower is the reverse flow stress since τ_{BK} is in opposite direction. This can account for the Bauschinger effect. Embury^[1,20] presented an alternative way to explain the flow stress by introducing three terms: σ_o , the basic flow stress; σ_{BK} , the back stress; and σ_{for} , the forest hardening effect (dislocation interactions). Since the back stress, σ_{BK} , opposes the flow in the forward direction and assists the flow in the reverse direction, therefore, we could have:

$$\sigma_F = \sigma_o + \sigma_{for} + \sigma_{BK} \quad (1.2)$$

$$\sigma_R = \sigma_o + \sigma_{for} - \sigma_{BK} \quad (1.3)$$

Where σ_F and σ_R are forward and reverse flow stresses, respectively. In order to have the back stress assisting the reverse loading, the dislocations moved forward must remain in the same position as they were before unloading. Mott assumed that the stress concentration around dislocations would give rise to plastic deformation by slip on intersecting slip planes. The dislocations mobilized on these planes would combine with those dislocation clusters that formed and piled up at strong barriers in prestrain to form Lomer-Cottrell locks. The latter represents a nonmobile dislocation that impedes the motion of other dislocations on

their respective planes, therefore, would prevent the pile-ups from running back when the load is removed.

The second approach of dislocation theory to explain the Bauschinger effect was proposed by Orowan^[1,12]. The preliminary results from his group in MIT, covering copper, aluminum, brass, nickel and magnesium, drew attention to the facts that: first, at reversal of deformation the entire stress-strain curve shifts in the negative stress or positive strain direction and the stress-strain relation changes its characteristic parabolic form, and actually there is a permanent softening of the material rather than the Bauschinger effect. A permanent softening has in fact been observed, but its magnitude indicates that the back stress effect is relatively small. Heating of unloaded but prestrained specimens reduces their stress-strain related anisotropy, and after heating the specimens to the above recrystallization temperature, all traces of the Bauschinger effect disappear. The above results led Orowan to the following conclusion. Considering the small value of permanent softening for copper (2.75 MPa after approximately 34.5MPa prestress,) the back stress alone cannot account for the Bauschinger effect. Orowan suggested that there must be some other mechanisms contributing also. He, therefore, discussed this problem in terms of the effects of two generalized types of obstacles to slip namely strong obstacles and permeable obstacles. The former were expected to promote back stress hardening because dislocation rings, Orowan loops, were formed when dislocations under applied stress tend to sweep through the obstacles and form dislocation pile-up in front of these obstacles. The back stress hardening in this case must be wiped out largely by reversed plastic deformation, a circumstance which gives rise to permanent softening. On the other hand, an array of permeable obstacles could produce low initial flow strength in the reverse direction without causing appreciable

permanent softening. In this case, it was envisaged that mobile dislocations would move forward through the obstacles array at a lower flow stress, breaking through individual obstacles under the pressure of very few dislocation pile-ups. At the end of prestraining, most dislocations would reach a point where they were held up against a particular row of obstacles, generally closed spaced. On stress reversal, the dislocations would move back from the row of obstacles, and this movement would start at a relative low applied stress, but in the absence of extreme dislocation pile-ups. The flow stress would increase rapidly towards the value obtained in prestraining since the dislocations would encounter another row of closely spaced obstacles, see Fig.1.4. This mechanism is most prevalent in metals which have numerous barriers to dislocations movement such as polycrystals (grain boundaries) or dispersion hardened metals (with particulate). In other cases, a dislocation line can be seen interacting with a series of immobile defects. When immobile dislocations are closely spaced, they are called "forest dislocations". The sessile defects may be point defects (vacancies or interstitial atoms), small particulates, or immobile dislocation lines (perpendicular to the paper) which are not active in the current orientation. At maximum load (as given by the solid line), the line dislocation is blocked by point defects, but the line bows out under the applied stress. When the load is removed, the line rebounds (as given by the dotted line) to reduce energy. It is well known that line dislocation energy is proportional to the square of the length of the line. Again, the rebound will produce a small amount of deformation in the direction opposite to the initial plastic deformation, adding to the anelastic effect. When the load is reversed, there will be an area containing relatively few barriers to dislocation movement, and causing a lower yield point. This mechanism has been called the forest and glide dislocation approach and is most prevalent in alloys and metals which have been

quenched from a high temperature (in this case there will be a large percentage of vacancies present). Another aspect of this mechanism is that upon reverse loading, dislocations will annihilate dislocations of opposite sign when they come into contact, thus reducing strain hardening and the yield point of the material on reverse loading. This mechanism will occur in alloys where a second phase is present, and in dispersion hardened metals. As mentioned previously, dislocations of opposite sign will interact to annihilate each other. In addition, other dislocations can interact to form jogs in the dislocation line, rendering that part of the dislocation immobile. Once a dislocation has been rendered immobile by interaction, it no longer contributes to the Bauschinger effect in the material because it is no longer available to contribute to the backstress in a dislocation pileup. Thus, only reversible (mobile) dislocations can contribute to the Bauschinger effect. As the plastic strain increases, dislocation density increases, and the change for dislocation interaction increases. However, as new dislocations are always being generated during plastic deformation, a saturation value will be reached where there will be a constant fraction of mobile and immobile dislocations in the material as plastic deformation is increased. Therefore, it is expected that a saturation value of the Bauschinger effect will occur after a certain plastic strain is obtained.

1.4.3 Evaluation of the magnitude of the Bauschinger effect

One of the greatest difficulties with the Bauschinger effect is the evaluation of its magnitude. The difficulties relate to conceptual problems rather than technical ones. Attempts to describe the Bauschinger effect in terms of strain alone, such as those of Woolley (1953)^[1.11] and Buckley (1956)^[1.7], give rise to difficulties. They are typified by comparison of Abel's (1965)^[1.21] results with the results of experiments by Edwards and Washburn

(1954)^[1,22]. Edwards and Washburn obtained a high value of β , the Bauschinger strain, accompanied by a relatively small yield - stress lowering effect in zinc single crystals, while Abel's results show, for Al - 4% Cu crystals with θ or θ' precipitates present, a relatively small β value, but reverse yield stress which was so low that reverse yielding in fact occurred on unloading from the prestress. One may describe the zinc crystal as having a large Bauschinger effect and the Al-Cu alloy a much smaller effect using the Bauschinger strain as the criterion. However, in terms of yield stress lowering, the Al-Cu alloy exhibited by far the larger Bauschinger effect. Because of the many features that the effect exhibits, the evaluation remains varied. In the early investigations, an attempt was made to find better ways of describing and evaluating all aspects of the Bauschinger effect. For this purpose, the following parameters were proposed.

(1) **Bauschinger Strain β**

The gradual change from elastic to plastic deformation, as shown on a stress - strain curve, leads somewhat uncertainty in the actual magnitude of yield lowering during load reversal. Maybe this was one of the reasons why Woolley introduced the idea of Bauschinger strain, β . This strain is the total reverse strain that occurs during unloading and reverse loading at a σ stress level defined by $\sigma = - n\sigma_p$ where σ_p is the prestress. Woolley also proposed the use of another strain parameter ρ , defined as the ratio of the total (i.e. elastic plus plastic) reversed strain at $0.75 \sigma_p$ (called $\gamma_{0.75}$), to that at zero stress (γ_0), i.e. $\rho = \gamma_{0.75} / \gamma_0$. For a number of materials ρ varied from 2.85 to 4.3. In the absence of a Bauschinger effect, ρ would have the value 2.0. Buckley and Entwistle referred to the Bauschinger strain at $\sigma = - 0.75 \sigma_p$, Stotoz and Pelloux took the reverse strain at $\sigma = - 0.5 \sigma_p$, while Hsu and

Arsenault took $\sigma = -\sigma_p$. The last work, also referred to the Bauschinger strain factor and to the Bauschinger stress factor, indicated the limitations associated with the use of β . This can be further illustrated by the results of single crystals of Al - 4% Cu when GP zone or θ'' precipitations were present, the Bauschinger strain, β , at $\sigma = -0.75 \sigma_p$ was found to be zero when up to 1.0 % prestrain was applied. Edwards and Washburn showed on zinc single crystals that a relatively large value of Bauschinger strain was obtained with a relatively small yield stress lowering. On the other hand, Abel reported that, in Al - 4% Cu single crystals with θ' and θ precipitates, yielding occurred even during unloading, but because of rapid hardening during the reverse half cycle, β did not reach a large value. One can describe the zinc crystal as having a large Bauschinger effect and the Al - Cu alloy with θ and θ' precipitates as having a smaller effect by using the β criteria. However, they can be described equally well the other way around by using yield lowering as a criterion.

(2) Back Stress

As the yield lowering effect increasing with increasing prestrain, and increasing prestrain usually produces increased work hardening, the role of back stresses comes to the foreground for further consideration. Abel and Ham^[1,23] examined the possibilities of using back stress for the evaluation of the Bauschinger effect. The peak stress in the deformation of forward direction can usually be made simply in terms of the contributions from directional and non-directional components of hardening,

$$\sigma_p = \sigma_0 + \sigma_{for} + \sigma_{BK} \quad (1.4)$$

Where σ_p denotes the flow stress in forward straining and σ_0 is a derived value of the initial yield stress. σ_{for} represents the sum of contributions from the isotropic hardening

components. σ_{BK} is the mean directional stress, back stress. Assuming that the directional components of internal stress are not significantly relaxed in unloading, therefore, the sense of the strain reverse and reverse plastic flow will be assisted by σ_{BK} . It will be first observed at σ_R as a departure from elasticity. It might be expected that the flow stress at the outset of plastic deformation in reversed straining would be

$$\sigma_R = \sigma_0 + \sigma_{for} - \sigma_{BK} \quad (1.5)$$

In reality, stresses represented in σ_0 , σ_{for} , and σ_{BK} are not uniform on the scale of the microstructure. The plastic deformation will be initiated in reverse straining in regions where the back stress is particularly high in relation to the local flow resistance of the matrix. Usually a small amount of reversed plastic deformation occurs during unloading after forward prestraining and it continues to develop at infinitesimally small values of σ_R , but the initial hardening rate in reversed deformation is extremely high compared with forward flow. Combing the above two equations, σ_{BK} can be experimentally determined as:

$$\sigma_{BK} = (\sigma_P - \sigma_R)/2 \quad (1.6)$$

Orowan originally predicted that if flow resistance were caused by a permanent array of weak obstacles, which are permeable to dislocations, then the lowering of flow stress in reversed straining would be a transient effect. If dislocation pileups at strong obstacles are responsible for work hardening, then dislocation pileups inherited from forward straining would be wiped out and part of the strain expended in forward straining would be recovered in reverse straining. Therefore, permanent softening will be observed in Bauschinger test. Permanent softening is conveniently determined from a plot of the forward and reverse stress-strain curves in terms of absolute stress and absolute strain. Its value of $\sigma_P - \sigma_R$ is measured at a

reverse strain sufficient to give near parallelism between the two curves, see Fig. 1.2. This value of the flow stress difference is designated as $\Delta\sigma_p$. In more recent years, most of the estimates of σ_{BK} made directly from the Bauschinger effect have been made from measurements of $\Delta\sigma_p$. Atkinson measured $\Delta\sigma_p$ and followed the changes in dislocation substructures in copper crystals dispersion hardened with 0.3 - 1.0% volume fractions of oxide particles. They found that the calculated value of σ_{BK} based on theoretical relationship was close to $0.5 \Delta\sigma_p$.

$$\sigma_{BK} = 0.5 \Delta\sigma_p \quad (1.7)$$

In the last decade, the relationship has been assumed in making estimates of the contribution of the “back stress” to room temperature work hardening in polycrystalline alloys containing larger volume fractions of second phase particles. Bauschinger type experiments give much more information and there is a need to process that information more effectively in order to provide a better description and understanding of the phenomena which are involved. An attempt to achieve this was made by Abel when three Bauschinger parameters were introduced: a Bauschinger stress parameter β_σ , a Bauschinger strain parameter β_ϵ , and a Bauschinger energy parameter β_E , which are described at below.

A) **The Bauschinger stress parameter β_σ**

The Bauschinger effect was first defined as a yield lowering effect, the lowering of the elastic limit observed during straining in a particular direction as a consequence of a preceding plastic deformation in the opposite direction. In this proposed parameter the yield lowering is related to the prestress

$$\beta_\sigma = \Delta\sigma/\sigma_p \quad (1.8)$$

Where $\Delta\sigma$ is the yield reduction $\Delta\sigma = \sigma_P + \sigma_R$, in which σ_P is the peak forward stress and σ_R is the reverse yield stress. When plastic flow takes place during unloading or yield occurs before the load reaches to zero, σ_R would be a positive value so that the value of β_σ will be greater than 1.0. When plastic flow starts on reversal of the load, σ_R will be negative and the value of β_σ will be less than 1.0. This yield reduction can also be written as $\sigma_P - |\sigma_R|$, which is the two times of the value of the back stress σ_{BK} , therefore, the Bauschinger stress parameter is the measure of the total work hardening arising from the back stress and has the form

$$\beta_\sigma = \sigma_{BK} / 2 \sigma_P = (\sigma_P - |\sigma_R|) / 2 \sigma_P. \quad (1.9)$$

The smaller the value of β_σ , the smaller the Bauschinger effect.

B) The Bauschinger strain parameter β_ϵ

The Bauschinger strain parameter is defined as $\beta_\epsilon = \beta / \epsilon_P$ where β is the Bauschinger strain at $\sigma = -\sigma_P$, and ϵ_P is the plastic prestrain. When $\beta_\epsilon = 1.0$ the prestrain is fully reversed, and no strain hardening can take place. This would apply in the case of cyclic conditions at saturation. During cyclic hardening β_ϵ would be smaller than 1.0. A theoretical maximum of $\beta_\epsilon = 2.0$ is envisaged for the hypothetical case where during reverse deformation, all the mobile dislocations are displaced twice the distance covered during prestraining.

Up to this point, two parameters have been introduced. They are well defined in each case, but there are still some problems to define the magnitude of the Bauschinger effect. Take, for example, the previously mentioned result on single crystals of zinc and single crystals of Al - 4% Cu with θ' and θ precipitates. In the first case $\beta_\sigma < 0.7$ is associated with

$\beta_e > 0.7$, while in the second case $\beta_e > 1.0$ is associated with $\beta_e < 0.7$. Thus, it is not hard to conclude that neither stress nor strain derived parameters can provide an adequate measure of the Bauschinger effect in this particular case. A better approach appears to associate it with an area under the stress - strain curve. Such an area, which is shown shaded in Fig 1.2, may be taken to represent the energy saved in achieving a certain amount of deformation in reverse loading. It can be used to compare with the energy that would have been required to achieve the same increment of deformation in the absence of Bauschinger effect.

C) The Bauschinger energy parameter, β_E

During deformation, an amount of the energy is stored in the specimen in the form of additional dislocations, point defects, etc. The fraction of this stored energy varies with the percentage of deformation introduced. Estimates put the fraction stored at very high deformation as 5 per cent. At lower deformation, the fraction stored is as high as 10 per cent at 10 per cent deformation, and it is very much higher at very small deformation. As the energy saved is defined as the Bauschinger energy E_S , the energy expended during prestrain is defined as E_P , and the ratio of these, $\beta_E = E_S / E_P$, is taken as The Bauschinger energy parameter. This measure of the Bauschinger effect reflects the stress or strain effect as well as the rapid work hardening during reverse loading. The recoverability or reversibility of the energy storage mechanisms associated with plastic deformation is the focus of this parameter. If plastic deformation takes place in the tensile direction up to σ_P , further tensile deformation would be expected to be an average flow stress of $(\sigma_P + \Delta\sigma)$. The average compressive reverse flow stress could be expected at $-(\sigma_P + \Delta\sigma)$ to complete the cycle in the absence of

the Bauschinger effect. However, the fact that the actual average flow stress at full stress reversal σ_R is $-(\sigma_P - \Delta\sigma)$ due to the Bauschinger effect. This means that an amount of plastic deformation is achieved with a smaller amount of work input during stress reversal than is the case of reloading in the same sense from zero stress. This saving is related to that part of the stored energy that is elastic in nature and is recoverable with stress reversal. This saved energy can be approximately estimated as $E_S = (\sigma_P - \sigma_R) \beta$, that is, the expected minimum energy required for achieving β amount of strain without Bauschinger effect minus the actual energy expended in achieving β amount of strain with Bauschinger effect. It is suggested that this saving occurred because the elastic energy accumulated during the tensile deformation was stored in a reversible way and was given out by the system during compression. This could result in a corresponding reduction in the work done on the system. If one takes this further and considers that the prestraining flow curve, relating to E_P , can be envisaged as $\sigma_P = \bar{\sigma}_{FOR} + \bar{\sigma}_{BK}$ by using average values for the frictional and back stress components, the reversibly stored energy could be limited to the value of $\sigma_{BK} \epsilon_P$, where ϵ_P is the plastic prestrain. The average value of back stress $\bar{\sigma}_{BK}$ here represents all the elastic stresses built up by dislocation interactions. Thus it may be written as $E_S \leq \sigma_{BK} \epsilon_P$ and therefore β_E will have a limiting value defined by

$$\beta_E = E_S/E_P = \bar{\sigma}_{BK} \epsilon_P / \bar{\sigma}_P \epsilon_P = \bar{\sigma}_{BK} / \sigma_P = 1 - \sigma_{FOR} / \sigma_P. \quad (1.10)$$

In this way, the Bauschinger effect is a direct measure of the average elastic stress built up during the previous, and directionally opposite deformation cycle. It gives an insight into the nature of deformation processes during prestrain. Very low values of β_E would indicate deformation processes corresponding in a theological model to a rigid - plastic material

where the energy input of a deformation cycle would be used up in kinetic friction. Larger β_E values would correspond with deformation processes where a larger fraction of the energy input is stored in a recoverable manner. During reverse loading or even during unloading, the initial departure from a response defined by the elastic modulus of the material is a manifestation of this recoverably stored energy.

For the evaluation of the Bauschinger effect, the three parameters when used together offer the most comprehensive assessment.

1.5 Effect of Silicon on tempering of spring steels

1.5.1 The significance of silicon content in the spring steels

As being mentioned before, one of the most effective ways of improving the fuel economy of an automobile is to reduce the weight of its parts. This demand certainly brings the sag resistance of spring steels into the foreground. To meet this demand, the most efficient and simplest way is to raise the hardness by strengthening the matrix of the material. For a given carbon content and alloy composition, the final heat treatment (tempering treatment) establishes the hardness of the steel. The new spring steels that have been developed recently take advantage of higher silicon levels as well as additions of microalloying elements. Silicon known as a solid solution strengthener is also effective in refining carbides that formed during tempering. Evidence showed that silicon affects hardness during the tempering of spring steels. A review of the literature gave an indication that silicon retarded softening in the tempering through its effect on the ϵ -carbide - cementite transition. Because of its beneficial effect, Si was found to be the most important factor to improve sag resistance of spring steels. Borik^[1,24] used stress relaxation tests to

study the effect of Si on sag resistance of spring steels. Results showed that increasing the Si content, in the range of 0.29 to 2.26wt pct, increased the sag resistance of the steels. There is no exception from Furr's work. His Bauschinger twist test result demonstrated that both C and Si improved the relaxation resistance of steel. In addition, Tata's^[1.25] static and dynamic tests, Kawakami's^[1.26] Bauschinger torsion test, and Ohara's^[1.27] research further confirmed that Si improves the sag resistance of spring steels with increasing Si content up to 2.2 pct.

1.5.2 Tempering of Steels

As we have known, steels that have subjected to a hardening quench usually undergo specific volume changes because of the transformation of austenite to martensite. Of more general importance is the fact that a structure that is almost completely martensite is highly supersaturated with carbon, extremely brittle, and very likely to develop quench cracks. These factors lead to the conclusions that steels with quenched martensite structure are of little useful value, and a tempering treatment needs to be followed to improve the physical properties of quenched steels. In a tempering process, the temperature of the steel is raised to a value below the eutectoid temperature and held there for a certain period of time, after which the steel is cooled to room temperature. The obvious intent of tempering is to allow diffusion process time to produce both a dimensionally more stable structure and one that is inherently less brittle. Based on x-ray dilatometric analysis and studies of microstructure, the tempering generally takes place in four distinct and overlapping stages.

(a) Stage one. 100 - 250 ° C: Precipitation of transition carbides, ϵ - carbide, and lowering of the carbon content of martensite.

(b) Stage two. 200 - 300 ° C: Decomposition of retained austenite. Retained austenite transfers to ferrite and cementite.

(c) Stage three. 200 - 350 ° C: Replacement of ϵ - carbide and low - temperature martensite by cementite and ferrite.

(d) Stage four. Above 350 ° C : Cementite coarsens and spheroidizes; recrystallization of ferrite.

In fully hardened martensite, the carbon is almost entirely supersaturated in solid solution in a body - centered tetragonal lattice and in this condition, internal stresses are high. On tempering, carbides are precipitated, and iron atoms of the lattice are rearranged, thus providing considerable stress relief. The carbide that precipitated during the first stage of tempering has a composition between that of Fe_3C and that of Fe_2C and has been called ϵ -carbide. It starts to show up at 100 ° C and subsequently decomposes to cementite at higher temperature. When the carbide of first stage precipitates from martensite, it is sometimes accompanied by a slight increase of hardness. This hardening due to the formation of ϵ -carbide is accompanied by softening because carbon is simultaneously removed from the martensite matrix. Whether softening or hardening occur depends on the amount of carbide that precipitates, but marked softening occurs at higher tempering temperature that is mainly due to the formation of cementite and complete carbon depletion of the martensite.

As tempering temperature is raises to about 250 ° C, the martensite atomic lattice is breaking down and internal stress gets relief. This, therefore, results in some degree of improvement in terms of toughness and ductility. The ratio of yield strength and ultimate tensile strength is also increased because of this improvement. On the other hand, there is, for most steels, an intermediate range of temperature that can cause loss of toughness. This is

called martensite embrittlement and the degree of embrittlement occurring within it varies with the alloy content. It has been suggested that this embrittlement, which generally reaches its maximum on tempering at about 350 ° C, is associated with the resolution of ϵ -carbide and the precipitation of cementite films along martensite plate boundaries. Further increase of the tempering temperature above the embrittlement range could cause softening of the matrix due to carbon depletion. This can lead to an increase in ductility that eventually overcomes the embrittlement effect of the cementite films. As the tempering temperature reaches higher range, the coalescence of carbides causes a further increase in ductility and toughness. The cementite initially formed during the tempering containing high percentages of carbide-forming elements tends to change gradually to more stable alloy carbides. How fast these changes can occur depends on the rate of diffusion of carbon, more particularly on the rate of diffusion of alloying elements in the ferrite matrix. At the low temperature range, the diffusion rate is too low to enable the composition of the carbides to change significantly within normal tempering time. This change occurs only at the higher tempering temperatures or on prolonged treatment at intermediate temperatures. In low- and medium-alloy steels, however, formation of stable alloy carbides does not occur even after prolonged tempering at high temperatures, although the alloy content of the initial cementite increases as tempering progresses. The formation of carbides of increased alloy content leads to a diminution in the alloy content of the ferrite and it would be expected that this would reduce the strength of the ferrite matrix.

1.5.3 Effect of Silicon content on the tempering of spring steels

It is well known^[1.28, 1.29] that silicon strongly retards the softening of steels on tempering, thus permitting higher tempering temperatures to be used without severe loss in tensile

strength. Silicon also raises the temperature range in which the embrittlement occurs. Thus, silicon is added to certain high - performance steels to obtain an increase in strength with little impairment of ductility or impact toughness. Whatever the mechanism by which silicon retards the tempering processes, it remains of interest to further examine the steels which have silicon present. Owen^[1.30] did the study of general influence on the tempering of medium carbon steels by a magnetic method in 1952. His results clearly indicated that in the presence of silicon much higher tempering temperatures are necessary before any appreciable third stage decomposition can be detected. Higher tempering temperatures are required to complete the second and third stages. When the precipitation process is discussed, he concluded that carbon diffusion controls the kinetics of the second and third stages in plain carbon steels. However, when silicon content is sufficient, this control is no longer operative in the third stage, the reaction being controlled by the diffusion of silicon. The experimental data have also shown that the precipitates are spherical, tending to be rod - like or pearlitic in the high silicon steels, however, the precipitates tend to grow as plates in plain -carbon steels. He suggested that spheroidal precipitation in the silicon steels may be simply explained as being an influence of silicon content. The effective temperature range is raised because of high silicon concentration so that spheroidization rapidly takes place. In the terms of silicon diffusion phenomenon, Walter suggested a model to explain it. He assumed that the silicon content of the cementite is small compared with that of the matrix causing a build -up of silicon in front of the advancing interface. Then, for the precipitation to continue, silicon must diffuse from the interface to the matrix at the same time as carbon is diffusing in the opposite direction. There will be an interaction between the two diffusion processes. It seems that at low silicon concentration in alloy, carbon diffusion is the

controlling factor, but on increasing silicon content, a point is reached when the control transfers to the silicon diffusion process. Long tempering times of high temperatures are required to complete this transfer. It's no doubt that Dr. Owen's study is a valuable contribution to the literature on tempering, and helps greatly to clarify the manner in which silicon affects the tempering process.

Similar works were carried out by Hobbs, Lorimer, and Ridley^[1.31] from university of Manchester in 1972. They have studied the effect of additions of 1% and 2% silicon on the microstructure of quenched and tempered medium - carbon steels by using TEM that provided more evidence about the effect of silicon on tempering. The results showed that addition of silicon markedly retarded the tempering process. The retardation was mainly associated with a slowing down of the growth of cementite particles and a retardation of the process of dislocation annealing. In addition, the particle sizes were smaller at any tempering temperature when silicon was present.

Based on all the previous studies, it is clear that addition silicon markedly retarded the tempering process, therefore, changed the carbide size, shape, and distribution in steels. These differences in characteristics of the carbides are related to the different silicon contents of the steels. The characteristics of the carbides are major factors in determining the microyield properties and, thereby, the relaxation characteristics of the spring steel.

1.6 Objectives

The objectives of the present investigations were: (1) To determine or characterize the sag or relaxation behavior of standard and microalloyed spring steels. (2) To investigate how the level of hardness of spring steels affects the magnitude of Bauschinger effect in terms of Bauschinger stress parameter, and therefore, the sag behavior of spring steels. (3) To examine the effect of silicon content on the microstructure of quenched and tempered spring steels, and therefore, on the Bauschinger effect and sag behavior of spring steels. The morphology of the carbide formed during tempering and silicon distribution after tempering treatment was given a closer examination.

In this project, three spring steels which are either being commercially used or being newly developed were selected; namely, SAE grades 5160H, 9259V, and Duraspring steels respectively. All the Bauschinger effect tests used to evaluate sag resistance were carried out in a tension- compression mode with a universal MTS testing machine. Since the outputs of conventional tensile and compression tests can be, in principle, easily converted to test - piece -independent stress - strain curves, a particular value of the reverse yield stress could be determined. The Bauschinger test results can also be compared without the influence of specimen sizes.

1.7 References

- 1.1. K. Kawasaki, Y. Seto, T. Yamazaki, and T. Hijikata, "Properties of Induction Heat-Treated High-Strength Spring Steels", SAE Technical paper Series, 830656, 1983.
- 1.2. S. T. Furr, "Development of a New Laboratory Test Method for Spring Steels", Transaction of the ASME: Journal of Basic Engineering, 94, 1972, pp. 223-227.
- 1.3. A. Brownrigg, and T. Sritharan, "Spring Steel Hysteresis", Materials Forum, 10, 1987, pp.58-63.
- 1.4. A. Abel, "Historical Perspectives and Some of the Main Features of the Bauschinger Effect ", Materials Forum, 10, 1987, pp.11-25.
- 1.5. J. Bauschinger, "MECHANISCH-TECHNISCHEN LABORATORIUM", Materials Forum, 1886.
- 1.6. A. H. Cottrell, "Dislocations and Plastic Flow in Crystals", 1953 (Oxford University Press), pp.111 and 132.
- 1.7. S. N. Buckley, and K. M. Entwistle, Acta Metall, 1956.4, pp.352.
- 1.8. H. G. Van Bueren, Imperfections in Crystal, 1960 (Amsterdam), pp.240.
- 1.9. G. E. Dieter, Mechanical Metallurgy, 1961 (McGrawHill), pp112.
- 1.10. F. A. McClintock, and A. S. Argon, Mechanical Behavior of Materials, 1966 (Addison-Wesley), pp185.
- 1.11. R.L. Woolley, Philos. Mag, 44, 1953, pp. 579.
- 1.12. E. Orowan, "Cause and Effect of Internal Stresses - Internal Stresses and Fatigue in Metal", Symposium, Detroit, 1958.
- 1.13. E. Heyn, Metall and Erz, Heft 22, 22, November 1918, pp.441-2 and 436-41.

- 1.14. G. Masing, *ibid.*, 1926.5, pp.135
G. Masing, and W. Mauksch, *ibid.*, 1926.5, pp.142.
- 1.15. E. Schmid, and W. Boas, *Plasticity of Crystals*, London, 1950 (Hughes & Co.).
- 1.16. Z.Wang, and H. Margolin, "The Interaction of Surface and Interior to Produce Bauschinger Behavior in 70-30 α -Brass Single Crystal Oriented for Easy Glide", *Res Mechanica*. 21, 1987, pp.249-286.
- 1.17. N. F. Mott, *Phil. Mag.* 43, 1952, pp1151.
- 1.18. A. Seeger, *Dislocation and Mechanical Properties of Crystals*, John-Wiley and Sons, New York, 1957, pp. 243.
- 1.19. L. M. Brown, "Orowan's Explanation of the Bauschinger Effect", *Scripta Metallurgica*. 11, 1977, pp.127-131.
- 1.20. J. D. Embury, "Plastic Flow in Dispersion Hardened Materials", *Metallurgical Transactions*. 16A, 1985, pp2191-2200.
- 1.21. A. Abel, 1965, MSc thesis, McMaster University, Canada.
- 1.22. E. H. Edwards, and J. Washburn, *ibid.*, 1954, pp.1239.
- 1.23. A. Abel, and R. K. Ham, *Acta Metall.* 14, 1966. pp.1489.
- 1.24. F. Borik, V. A. Biss, and Y. E. Smith, "Sag Resistance of Si-Mo and Si-Cr Spring Steels", Paper 790409 presented at SAE Congress and Exposition, Detroit, March 1979.
- 1.25. H. J. Tata, E. R. Driscoll, and J. J. Kary, "Steels for Automotive Coil Springs with Improved Resistance to Relaxation", Paper 800480 presented at SAE Congress and Exposition, Detroit, Feb. 1980.

- 1.26. H. Kawakami, Y. Yamada, S. Ashida, and K. Shiwaku, "Effect of Chemical Composition on Sag Resistance of Suspension Spring", SAE Technical Paper Series 820128, Feb. 1982.
- 1.27. M. Ohara, K. Chishima, and K. Uchibori, Mitsubishi Steel Manuf. Tech. Rev., 1981, vol. 15, pp.13-20.
- 1.28. W. S. Owen, Trans. ASEM, 1954, vol. 46, pp.812-29.
- 1.29. A. G. Allten, and P. Payson, Trans. ASME, 1953, vol. 45, pp. 498-532.
- 1.30. W. S. Owen, Paper presented before the Thirty-fifth Annual Convention of the Society, Cleveland, October 17-23, 1953.
- 1.31. R. M. Hobbs, G. W. Lorimer, and N. Ridley, "Effect of Silicon on the Microstructure of Quenched and Tempered Medium-Carbon Steels", JISI, Oct. 1972,pp.757-764.

Chapter 2

2.1 Materials

The materials have been selected for this project were SAE 5160H, 9259V, and Duraspring steels. The chemical compositions of these steels used in this investigation with respect to the significant element are given in Table. 2.1. Other than the principal elements, the amount of any minor element present, such as S, P, N, Cu, etc. and their effects were considered insignificant. The 9259V, newly developed by STELCO Ltd., is generally called as chrome-silicon spring steel and has the highest carbon content among the three. The 5160H is a chromium steel and has the lowest silicon content but the highest chromium content. Duraspring steel (also known as 92V45), a new commercial alloy developed by Inland Steel Ltd., has the highest silicon and manganese content. All the materials received were in the hot - rolled condition. The 5160H was hot - rolled to 10.0mm thick plate and 9259V as well as Duraspring steel were hot - rolled to 16 mm and 13.5mm diameter bars respectively.

Table 2.1. Chemical Composition of the Steels Investigated. Wt. %

| GRADES | C | Mn | Si | Cr | V |
|------------------|------|------|------|------|------|
| 5160H | 0.55 | 0.76 | 0.28 | 0.75 | 0.01 |
| 9259V | 0.61 | 0.87 | 0.88 | 0.52 | 0.10 |
| Duraspring Steel | 0.47 | 1.28 | 1.22 | 0.53 | 0.15 |

The difference in carbon concentration among these three steels is relatively small. By contracts, the difference in silicon content among three steels appears to be more significant, especially between 5160H and Duraspring steels. Generally speaking, alloying element Si concentration is added to improve the relaxation resistance of spring steels and to further utilize its solid solution hardening effect^[2.1, 2.2]. The Mn improves the hardenability of spring steels. The Cr improves ductility and surface finish of spring steels. The V is good for grain refinement. The strengthening by precipitation of alloy carbides of Cr, V, etc., often referred to as secondary hardening, is also well known^[2.1, 2.2].

2.2 Test sample preparation

2.2.1 Test specimen

The test specimens used for both tensile test and Bauschinger test are cylindrical shape with threads on both ends. The dimensions of specimen are given in Fig 2.1.

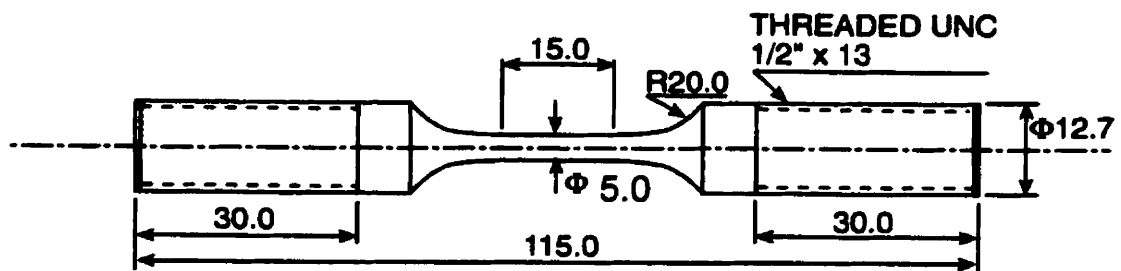


Fig. 2.1 Specimen dimensions for all the tension and Bauschinger effect tests (all dimensions in mm).

The configurations of test specimen are based on the ASTM standard ^[2.3]. According to ASTM, the selections of test specimen orientation relative to the rolling direction of products and specimen location are both taken into considerations. Orientation is important to standardize test results relative to the directionality of properties that often develops in the microstructure of materials during processing. Some causes of directionality include the fibering of inclusions in steels, and the formation of crystallographic textures in most metals and alloys. The location where a test piece is taken from is an important factor because the manner in which a material is processed influences the uniformity of microstructure along the length of the product as well as through its thickness or cross section. For the consideration of those factors mentioned above, all the test specimens were taken from midway of either plate or round bar along the rolling direction. All the test specimens received from machine shop met the size specifications provided to the machine shop. To ensure dimensional accuracy, however, each test specimen was measured prior to further treatment or testing.

2.2.2 Heat treatment

For a typical spring manufacturing process ^[2.4], the bar of the spring steel is austenitized for about half hour at a certain temperature, hot-wound into springs, quenched in oil, followed by tempering springs to a specified hardness, shot-peening, and then mechanically set by compressing the spring to the fully closed position. For the same reason, all specimens used for testing were subjected to the similar quenching and tempering cycles prior to the test. Fig 2.2 is the schematic representation of the heat treatment process.

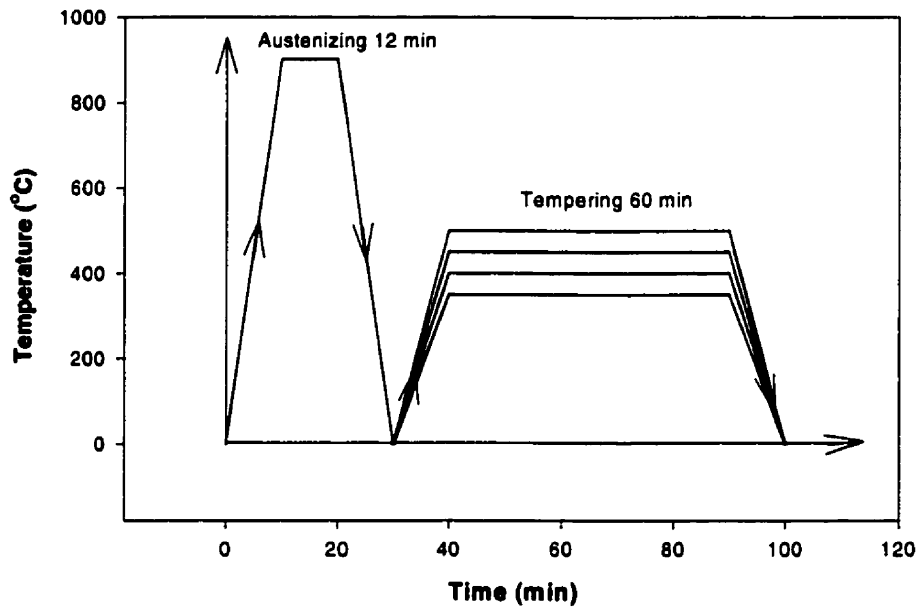


Fig 2.2 Heat treatment cycles for 5160H, 9259V, and Duraspring steels.

All specimens were austenitized for 12 min at 905 °C in a LindBerg Hevi-duty furnace followed by oil quenching into Vitrea 22, a 5-weight mineral oil with a fast heat dissipation rate. Tempering, always for 1 hour, was done in the same furnace and in the temperature range of 250 °C - 550 °C to achieve desired hardness levels for all three steels. For a better temperature control of the furnace, an additional thermocouple was used to monitor the temperature closely (± 0.5 °C). The tip of the thermocouple was placed near the specimen in the furnace so that it was exposed to the same heating environment as the specimen and one can get the accurate readings. Extra caution was taken to quench the specimen vertically, along the axis, so that thermal stresses would not cause any warping.

The required tempering temperatures for certain hardness levels were interpolated from tempering curves established by heat treating a series of specimens at different temperatures. These tempering temperatures cover the desired hardness levels traditionally employed for suspension coil springs in automobile industry.

After the heat treatment cycle, all specimens were carefully polished to obtain a smooth, flaw-free surface for the strain gauge to rest against. The reason for polishing is that machining grooves left on the specimens may inhibit movement of the knife edge of the strain gauge, giving inaccurate readings. In addition, machining introduces surface strain which may affect the results. More importantly, the specimens were exposed to air during heat treatment without any inert gas protection, therefore, the surface of specimen may be decarburized and oxidized to a certain degree. This poor surface quality would seriously affect fatigue life of springs because the maximum stress is at the surface. Optical microscope examination found that this decarburization layer is around 0.3 mm in depth right from the

surface. Without any hesitation, an approximately 0.5 mm thick layer was then removed from the gauge length by center grinding to ensure that above mentioned flaws were all eliminated.

2.2.3 Microstructure

All the samples for microstructure examination were also heat treated along with other specimens, mechanically polished, and finally etched in a 2% nital solution. The microstructures of these three steels after quenching and tempering were examined by using both optical microscope and scanning electron microscope (SEM).

2.3 Mechanical Testing

2.3.1 Hardness test

Hardness measurements after heat treatment were made on a calibrated Rockwell hardness tester on the C scale with the diamond indenter and 150-kg major load. The samples to be tested were polished to provide either free oxide and decarburization surface or smooth, flat surface perpendicular to the indenter. The measurement error is believed to be within ± 0.5 Rockwell C hardness point. Comparison of hardness values at different locations showed that there are no significant differences in hardness from center to surface on all three steels either after quenching or after tempering. Three or more hardness measurements were made for each specimen. In those few instances, where not all three hardness readings were identical, additional hardness measurements were taken after regrinding and polishing.

Hardness vs. tempering temperature curves, therefore, can be drawn for these three steels studied. The hardness vs. tempering curves certainly reveals significant amounts of information about the tempering behavior of these spring steels. Each data point represented an average value of three hardness readings on the same sample.

2.3.2 Material Testing System

A 100 kN MTS (Material Testing System - model number 630) testing machine was used for all the tensile tests and Bauschinger effect tests. A half inch standard MTS extensometer (model number 632, 13B-20) was calibrated first and attached to the specimen gauge length to measure the strain. Load measurement systems typically employ load transducers that are strain - gauge type load cells. Strain gauge is a device that undergoes electrical resistance changes in the presence of mechanical deformation. In this case, a load cell is connected to a bridge circuit to measure these minute resistance changes and thus the applied loads. The circuit is excited with a signal generated by the load cell amplifier, and an applied force causes the strain - gauge bridge circuit to be unbalanced. The resulting signal is returned to the amplifier and converted into an output signal (voltage) that is proportional to the applied force. The output can be read through a digital display on the load cell panel. The loads vs. displacement curves were recorded by a strip chart recorder on the MTS and through a data acquisition program that took direct voltage readings from the load cell and strain gauge.

2.3.3 MTS setup and procedures

Following steps are the procedures to set up the MTS test:

- 1) Measured the dimensions of the cross section at the center of the reduced section of a test specimen before loading the specimen onto the machine.
- 2) Set the machine in such a manner that zero force indication signifies a state of zero force on the specimen.
- 3) Threaded both upper and lower grips onto the specimen and attached to the upper holder of the load cell. Aligned the specimen properly.

- 4) Lowered the lower part of the specimen with grip into a base containing molten Wood's alloy (composed lead, tin, cadmium, and bismuth) and then cooled the base by letting cold water run through the base until Wood's alloy was solidified.
- 5) Attached the strain gauge to the gauge length of the specimen and zeroed.
- 6) Defined the speed of testing in terms of strain rate. Stroke control was used through all the tensile tests and Bauschinger effect tests, the strain rate was kept constant during the test. Strain rate is defined as $\dot{\epsilon} = d\epsilon / dt$, and is conventionally expressed in units of s^{-1} , i.e., "per second." The spectrum available for "static" tension tests with hydraulic or screw-driven machine is between 10^{-5} to $10^{-1} s^{-1}$ [2.5]. In this case, all the tests were performed at room temperature at approximately a constant strain rate of $10^{-4} s^{-1}$.

2.3.4 Tensile test and Bauschinger test

For each grade of steel investigated, round tensile specimens were tempered to four hardness levels of 45, 47, 50, 54 HRc (± 0.5 HRc). Then, tensile tests were carried out throughout these hardness levels to determine the yield strength, ultimate tensile strength, and percent elongation to fracture. The engineering tension test is widely used to provide basic design information on the strength of materials [2.5]. The data obtained from the tension test are generally plotted as a stress – strain curve. From stress – strain curve, the limit of usable elastic behavior is described by the yield strength. The yield strength is defined as the stress which will produce a small amount of permanent deformation, generally equal to a strain of 0.002. Plastic deformation begins when the elastic limit is exceeded. As the plastic deformation of the specimen increases, the material becomes stronger (strain hardening) so that the load required for extending the specimen increases with further straining. Eventually the load reaches a maximum value. The maximum load divided by the original area of the

specimen is the ultimate tensile strength. The conventional measures of ductility that are obtained from the tension test are the engineering strain at fracture, usually called the elongation or the reduction of area. Both of these properties are obtained after fracture by putting the specimen back together and taking measurements of gage length and cross section area. The tensile properties were all listed in a table for three steels at a certain hardness level. Each data listed in the table is an average value of three tests on the same material and the same testing condition.

Bauschinger hysteresis loop in tension - compression model was generated by loading the specimen in tension beyond its macroscopic yield point to a specific stress level, unloading to the zero stress level, and then immediately reloading the specimen in the compressive direction to the same stress level as was achieved in the tensile direction. The reverse yield stress along with the forward peak stress were used for the computation of the Bauschinger stress parameter, a parameter defined for evaluation of the magnitude of Bauschinger behavior. Pre-plastic strain and strength in terms of hardness of the specimen tested were varied, therefore, Bauschinger stress parameter vs. pre-plastic strain and hardness curves could be deduced. Each data point displayed on the curves represented an average value of two tests carried out at the same condition.

2.4 Reference

- 2.1. H. C. Keysor, *Product Eng*, 1946, vol.17. pp.86-89.
- 2.2. A. S. Kenneford, G. C. Ellis, *J. Iron Steel Inst.*, 1950, vol. 164(1), pp. 265-77.
- 2.3. **Standard Test Methods for Tension Test of Metallic Materials, Designation: E 8 – 95a**, *Annual Book of ASTM*, vol. 14.02, 1995, pp.56.
- 2.4. T. Murai, S. Takamuku, and N. Taenosita, “High Sag Resistance Spring Wire for Automotive Suspension”, *SAE Technical Paper Series 850059*, 1985.
- 2.5. G. Deiter, *Mechanical Metallurgy*, New York,1976, pp.275.

Chapter 3

3.1 Tempering behavior

Table 3.1 shows that the hardness right after the quenching for three steels investigated.

Table 3.1 As quenched hardness of 5160H, 9259V, and Duraspring steels.

| HARDNESS | 9259V | 5160H | DURASPRING STEEL |
|-----------------|--------------|--------------|-------------------------|
| HRc | 61.2 | 59.6 | 58.5 |

As we have known, the 9259V had the highest carbon content among three steels, followed by 5160H and then Duraspring steel. After quenching, the hardness of as – quenched materials showed exactly the same order, see table 3.1. Thus, the hardness obtained in quenching condition depends almost exclusively on the carbon concentration. Additional alloying elements, such as Si and Mn, have no significant effect on the hardness after quenching process.

Systematic experimental work on the hardness vs. tempering-temperature relationship was carried out with these spring steels. The hardness for all tempered specimens was influenced when additional alloying elements, such as silicon, presented in these three steels. The effect of the alloying elements in resisting softening on tempering can be observed. The degree of resistance to softening showed on these curves is varied with tempering temperature and composition.

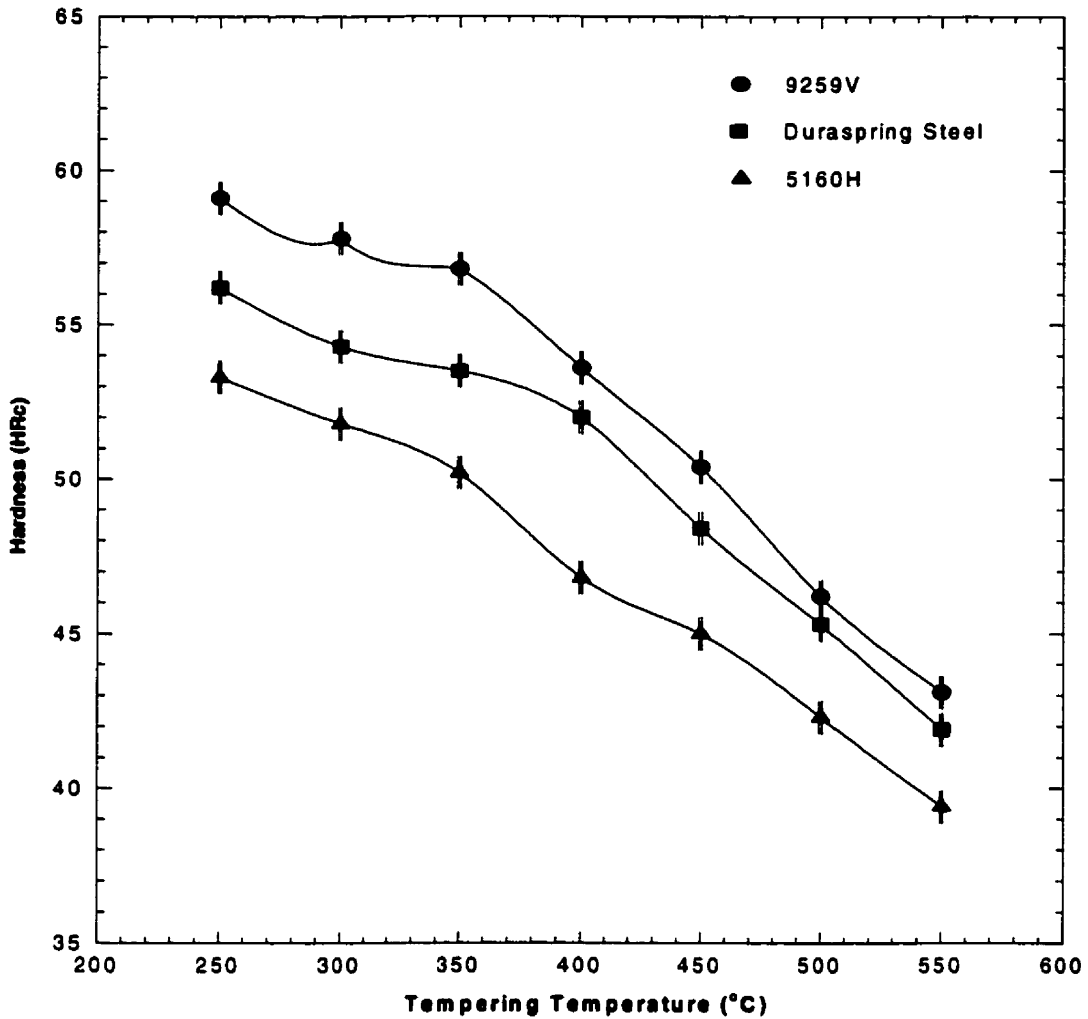


Fig 3.1 Hardness vs. tempering temperature curves for 5160H, 9259V, and Duraspring steels.

From Fig 3.1, the following facts were observed.

- (1) A general trend of softening with increasing in tempering temperature is obvious. For a constant tempering time of 60 min, after oil-quenching, the hardness of 9259V, 5160H,

and Duraspring steels decreases with increasing tempering temperature regardless of major difference of silicon content and minor differences of other alloying elements.

- (2) The rate of hardness reduction is found to depend upon tempering temperature range for these three spring steels. At lower tempering temperatures, from 250 to 350 °C, the hardness decreases slowly. For Duraspring steel, this slow reduction is extended to a higher temperature, 400 °C. Above this temperature range, the rate of hardness reduction is actually greater for all three steels.
- (3) Under all the tempering conditions employed, 9259V still shows the highest hardness. The well known effect of silicon on tempering process is displayed by the higher hardness of the high-Si grades (Duraspring) at all tempering temperatures compared to the low-Si grades (5160H). This over all greater hardening tendency indicates that high silicon steels retard softening in the tempering to a somewhat better degree than low silicon steels.

3.2 Mechanical Properties

The conventional mechanical properties, such as 0.2 pct offset yield strength, ultimate tensile strength (UTS), can be measured on a stress-strain curve generated from a tension test. These properties may be altered by changing the tempering temperature. Table 3.2 lists these properties for three steels after being tempered to the same hardness level. As noted, both 9259V and Duraspring steels show significantly higher ductility than 5160H despite their similarity in strength. All the data listed below are an average value from three samples.

Table 3.2 Mechanical properties of 5160H, 9259V, and Duraspring steels at HRc 48

| GRADES | $\sigma_{0.2}$ (MPa) | σ_{UTS} (MPa) | $\sigma_{UTS}/\sigma_{0.2}$ | δ (%) | TOUGHNESS (KN/m) |
|-------------------------|--------------------------------------------|--------------------------------------------|-----------------------------------------------|------------------------------------|-----------------------------|
| 5160H | 1605 | 1715 | 1.07 | 6.5 | 479.25 |
| 9259V | 1595 | 1713 | 1.07 | 11.5 | 924.75 |
| Duraspring steel | 1606 | 1718 | 1.07 | 11.2 | 774.02 |

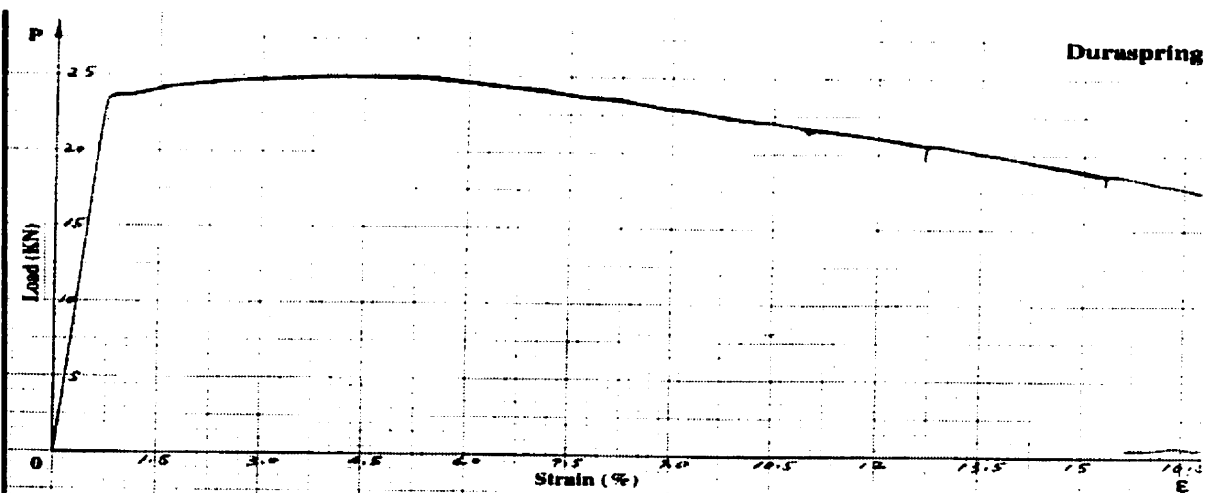
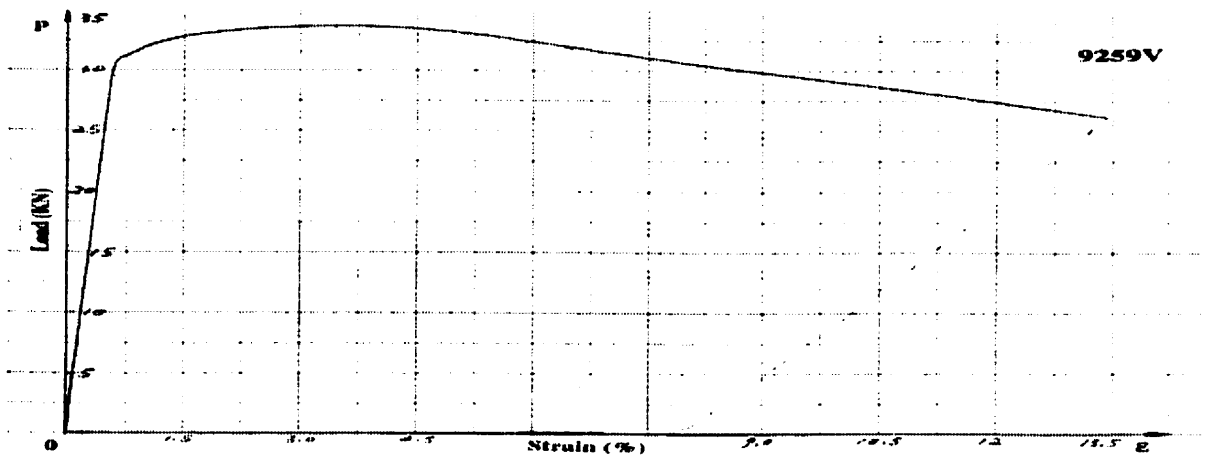
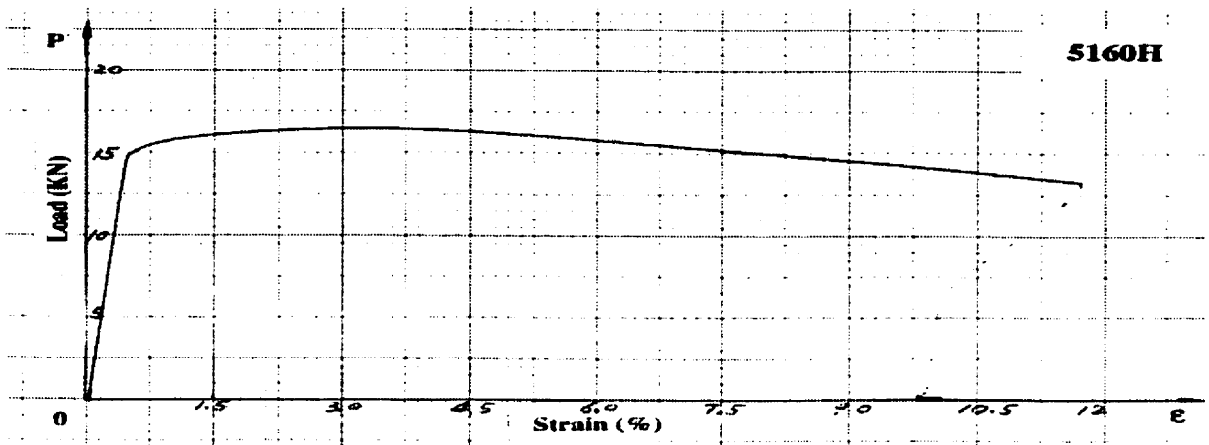


Fig 3.2. Stress-Strain curves for 5160H, 9259V, and Duraspring steels tempered to HRC 48 and tested at room temperature.

Fig 3.2 shows typical stress-strain curves of 5160H, 9259V and Duraspring steels. The general shape and magnitude of the stress-strain curve of a material are dependent on its composition, heat treatment, prior history of plastic deformation, and the strain rate, temperature, and the state of stress imposed during the testing. In this case, the composition and heat treatment are the only two variables. In the elastic region, stress is linearly proportional to strain. When the load exceeds a value corresponding to the yield strength, the specimen undergoes gross plastic deformation. The stress to produce continued plastic deformation increases with increasing plastic strain (strain hardening). The volume of the specimen remains constant during plastic deformation and as the specimen elongates, it decreases uniformly along the gauge length in cross-sectional area. Initially, the strain hardening more than compensates for this decrease in area and the stress continues to rise with increasing strain. Eventually, a point is reached where the decrease in specimen cross-sectional area is greater than the increase in deformation load arising from strain hardening. This condition will be reached first at some point in the specimen that is slightly weaker than the rest. All further plastic deformation is concentrated in this region, and the specimen begins to neck or thin down locally. Because the cross-sectional area now is decreasing far more rapidly than the deformation load is increased by strain hardening, the actual load required to deform the specimen falls off and the stress likewise continues to decrease until fracture occurs. This is exactly what happened during the tensile deformation of a specimen.

As one notes, the slope of the initial linear portion of the stress-strain curve, the modulus of elasticity or Young's modulus, from these three materials is similar. Generally the greater the modulus, the smaller the elastic strain resulting from the application of a given stress. The modulus of elasticity is determined by the binding forces between atoms. Since

these forces cannot be changed without changing the basic nature of the material, it is one of the most structure – insensitive of the mechanical properties. Logically, it will only be slightly affected by alloying elements, heat treatment, and any cold - work.

Once the stress exceeds the yield point up to the ultimate tensile strength, the specimen undergoes strain hardening. The strain up to maximum load is uniform strain. The flow curve of many metal materials in this region of uniform plastic deformation can be expressed by the simple power relation.

$$\sigma = K\epsilon^n \quad (3.1)$$

where n is the strain hardening exponent and K is the strength coefficient. σ and ϵ are true stress and true strain. They can be determined by engineering stress s and strain e .

$$\sigma = (P/A_0) \cdot (e+1) = s (e+1) \quad (3.2)$$

$$\epsilon = \ln (e+1) \quad (3.3)$$

A log-log plot of true stress and true strain up to maximum load will result in a straight line. The linear slope of this line is n and K is the true stress at $\epsilon = 1.0$. If the value of $n = 0$, it is a perfectly plastic solid. If the value of $n = 1$, it is a perfect elastic solid. For most metals n has values between 0.1 – 0.5. In this case, the value of n for 5160H, 9259V, and Duraspring steels tempered to HRC 48 are calculated as 0.15, 0.21, and 0.18 respectively. 9259V shows the greatest value of n . Strain hardening (also referred to as work hardening) results from a dramatic increase in number of dislocation – dislocation interactions and which reduces dislocation mobility. Therefore, larger stresses must be applied in order that additional deformation may take place. This indicates 9259V has the highest strain hardening effect followed by Duraspring steel and 5160H at this hardness level.

3.3 Microstructures

Fig 3.3 shows optical microstructures after oil quenching from 905°C for 5160H, Duraspring, and 9259V steels respectively.



Fig 3.3 Microstructures of 5160H, 9259V, and Duraspring steels oil quenched at 905 °C, 2% nital etch, 800×

In the as – quenched condition, all three steels showed fine lath martensite. The average lath length was ~ 0.5 μ m in 5160H, ~ 0.3 μ m in Duraspring steel, and was even finer, ~ 0.15 μ m in 9259V. The laths also appeared more tangled and shorter in 9259V. These variations in terms of martensite size were found to have insignificant effect on as – quenched hardness, see table 3.1.

Fig 3.4 showed optical microstructures of 5160H, 9259V, and Duraspring steels tempered at 250°C for 1 hour. The tempering took place under this temperature can be classified as stage 1, which is featuring the precipitation of ϵ - carbide and partial loss of tetragonality in martensite.



Fig 3.4 Microstructures of 5160H, 9259V, and Duraspring steels tempered at 250 °C for 1h, 2% nital etch, 800×

The optical microstructures examination revealed that the microstructures of these three steels under this tempering temperature were similar and consisted mainly of tempered martensite along with carbides and ferrite matrix. The martensite needles were smaller in the high silicon steel (Duraspring) than in the low silicon steel (5160H), with the 9259V having the smallest size of martensite. This may be a consequence of the smaller austenite grain size of the high-Si steels. The fact that the microstructures of 9259V and Duraspring steels were much lighter etching than 5160H. This indicated that the degree of rejection of carbon from martensite was smaller in 9259V and Duraspring steel than in 5160H. This would be expected as higher carbon content in 9259V also increasing the occupancy of the preferred interstitial sites, i.e. the octahedral interstices at the mid – points of unit cell edges, and centres of cell faces, thus reducing the mobility of the C atom. It is also likely that the presence of higher silicon content in both 9259V and Duraspring steels reduces the carbon activity involved in the precipitation of the epsilon carbide in the early tempering stage.

Fig 3.5 showed optical microstructures of 5160H, 9259V, and Duraspring steels tempered at 350°C for 1 hour. The second and third stages of tempering usually occurred in this temperature range. Generally, the retained austenite is decomposed; ϵ - carbide is replaced by cementite; and martensite loses its tetragonality.



Fig 3.5 Microstructures of 5160H, 9259V, and Duraspring steels tempered at 350 °C for 1h, 2% nital etch, 800×

The microstructures of all three steels tempered at this temperature showed similarity compared to the microstructures tempered at 250 °C. However, a little darker etching could be observed. This indicated that more carbon contents were rejected from the martensite. Again, it is not hard to find out that the martensite needles were smaller in the high silicon steels (9259V and Duraspring steels) than in the low silicon steel (5160H), probably in consequence of the smaller austenitic grain size of the former steels. The structures produced in the low silicon steel (5160H), after 1h tempers at temperature over 350°C, showed coarser carbides and more acicular patches of ferrite than seen in the high silicon steels (9259V and Duraspring steels). Fig 3.1 showed that Duraspring steel had a higher value of hardness at

this tempering condition than 5160H despite its lower carbon content. It indicates that silicon content affects the mean distance between particles which principally determines the hardness.

Further increasing the tempering temperature, the changes of microstructures became more obvious, see Fig 3.6. The tempering temperature above 450 °C indicates the fourth stage of tempering. Cementite coarsens and spheroidizes along with recrystallization of ferrite.



Fig 3.6 Microstructures of 5160H, 9259V, and Duraspring steels tempered at 450 °C for 1h, 2% nital etch, 800×

The optical metallographic examination revealed that the microstructures of three steels were similar and were composed of tempered martensite and ferrite matrix embedded with carbides. Among the three steels, there are significant differences in the size, shape, and spacing of the carbides after tempered at this condition. The carbides in the 9259V and Duraspring steels were small, spheroid, and closely spaced, whereas the carbides in the 5160H were much larger, rod-shaped, and widely spaced. These differences in characteristics

of the carbides are related to the different silicon contents in these spring steels. This phenomenon became more apparent after tempering at above 400° C range that is the third stage of tempering. Fig 3.6 also showed that more light – etching, acicular patches of ferrite presented in low silicon steel (5160H) than in the high silicon steels (9259V and Duraspring steels). These differences are attributed to a slightly a greater degree of completion of the third stage of tempering in the low silicon steels.

Fig 3.7 showed microstructures for all three steels tempered at 550°C condition.



Fig 3.7 Microstructures of 5160H, 9259V, and Duraspring steels tempered at 550 °C for 1h, 2% nital etch, 800×

Metallographic investigation showed that, in the higher silicon steels, carbides were smaller and more numerous and that the microstructures remained more acicular in appearance than in low silicon steels. These changes suggested that silicon content retards the coalescence of carbides, and allows carbides particles pinning the grain boundary. Consequently, these carbides may provide a resistance to grain growth. The combination of more and smaller carbides and an apparent lower state of recovery of the martensite (finer packets of ferrite)

causes the observed substantial increase in the hardness of tempered martensite as the percent of silicon in steel increases, see Fig 3.1.

3. 4 Bauschinger effect test

To quantify the change of the flow stresses upon stress reversal, a number of different parameters can be used. These parameters reflect the mechanisms involved in lowering the yield stress in the reversed direction. In the present study, one of these parameters, the Bauschinger stress parameter is employed to compare the internal stresses developed during the forward plastic deformation. The Bauschinger stress parameter reflects the fraction of the total work hardening arising from the back stress and has the form

$$\beta_{\sigma} = \sigma_b / 2\sigma_F = (\sigma_F - |\sigma_R|) / 2\sigma_F \quad (3.1)$$

Where σ_b is the back stress, σ_F is the forward flow stress, and σ_R is the yield stress upon reloading in the opposite direction. The larger the value of β_{σ} , the larger of the Bauschinger effect. In the present case, the Bauschinger stress parameter was plotted against pre-plastic strain and hardness respectively to characterize the Bauschinger behavior. Each data point was the average from three specimens heat treated and tested in the same way. It has been found that the Bauschinger behavior of three spring steels, namely 5160H, 9259V, and Duraspring steel, was investigated under different hardness levels and different pre-strain levels. The test results depend on not only the types of material tested, but also the deformation history, mainly pre-strain levels, see Fig 3.8.

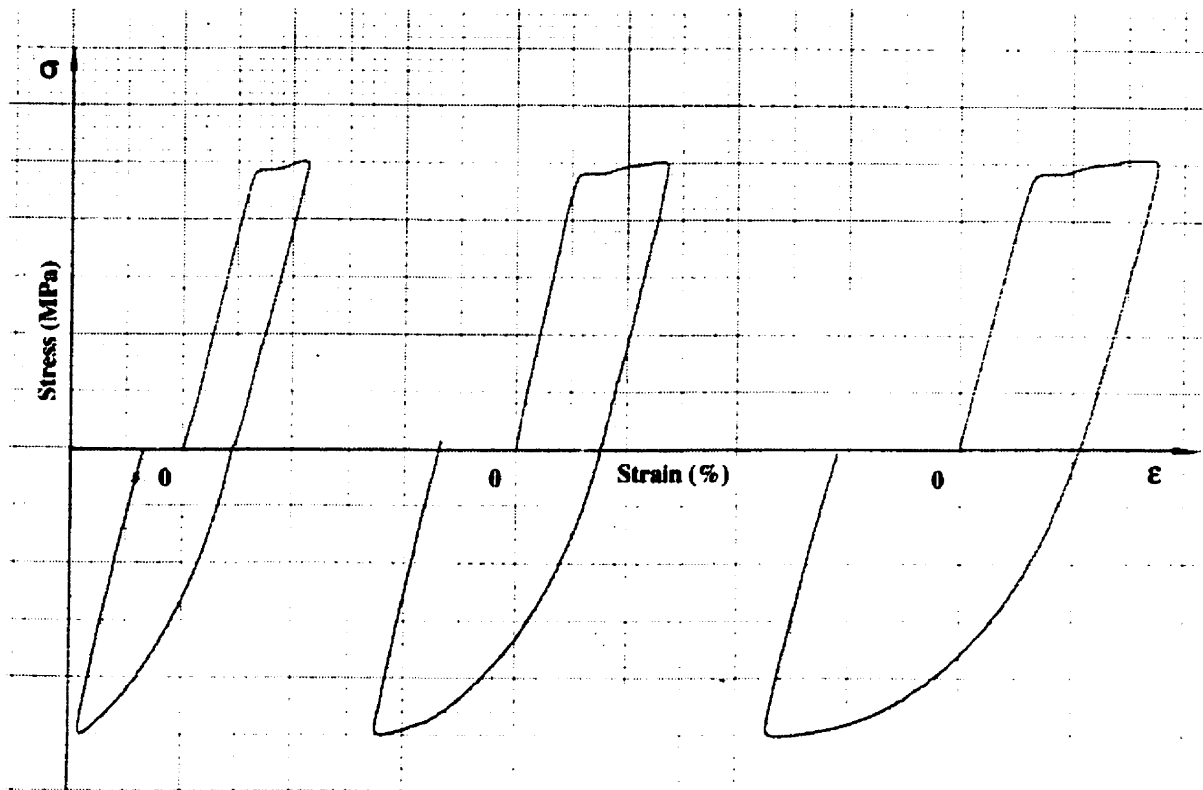


Fig 3.8 Schematic representation of room temperature Bauschinger effect tests for Duraspring steel tempered to HRC 48 at different pre-plastic strain levels

When the Bauschinger stress parameter was plotted against plastic pre-strain at different hardness levels, all three materials showed a similar trend, i.e. the Bauschinger effect increased with increasing pre-strain and then the rate of this increase gradually decreases until a saturation is reached at a certain pre-strain level, see Fig 3.9.

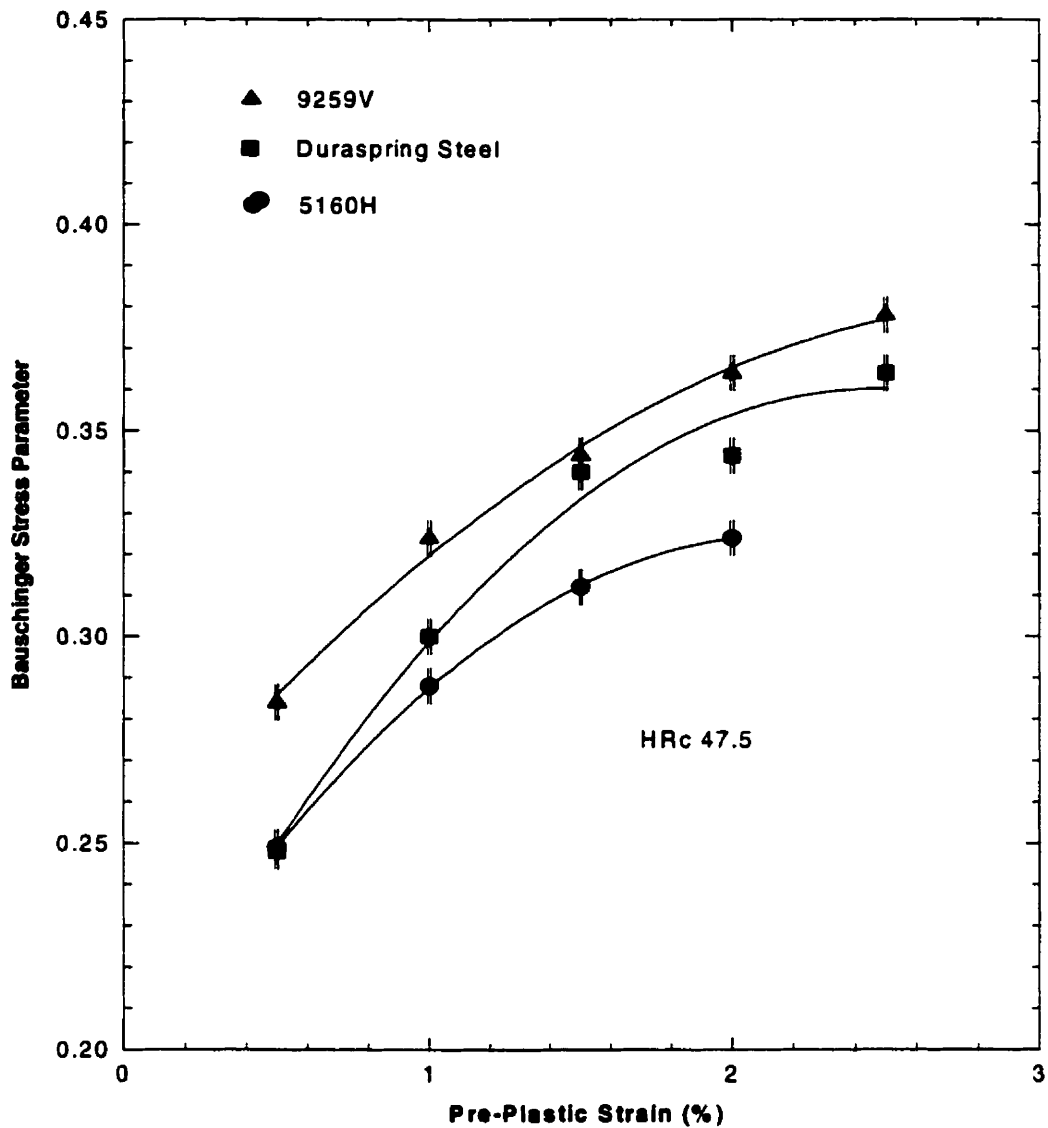


Fig 3.9 Bauschinger stress parameter vs. pre-plastic strain for 5160H, 9259V, and Duraspring steels on quenching – tempering condition.

The present results have also demonstrated that 9259V showed the highest Bauschinger effect. More interestingly, the high-Si Duraspring steel demonstrated a larger Bauschinger effect than the low-Si 5160H steel at all pre-plastic strain levels tested, although the former

has a considerably lower carbon content. The similar trend has been found at all different hardness levels, such as HRc 47 shown in Fig. 3.9.

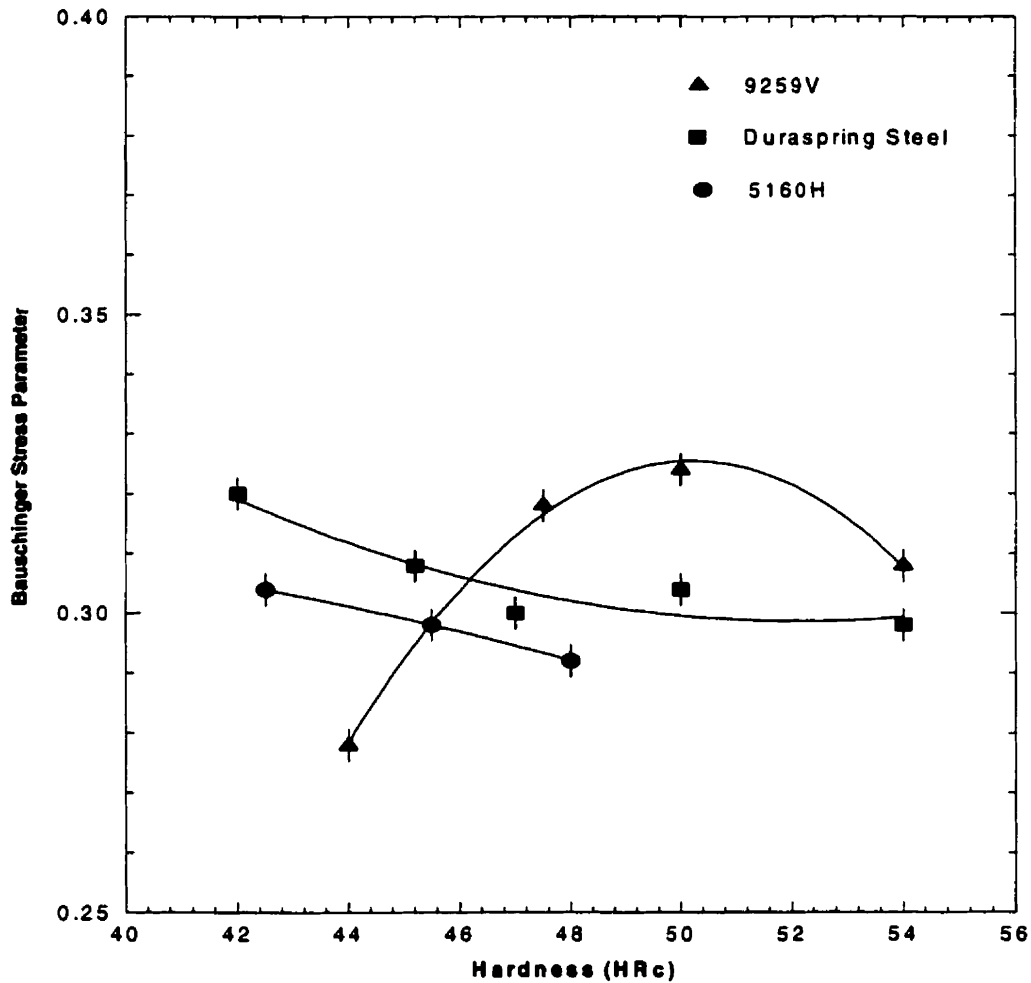


Fig 3.10 Bauschinger stress parameter vs. hardness curves for 5160H, 9259V, and Duraspring steels at 1% pre-plastic strain.

Bauschinger stress parameters at 1% plastic pre-strain have been determined and plotted against different hardness levels, as shown in Fig 3.10. Note that a maximum value of

Bauschinger stress parameter is found at around HRc 50 for 9259V steel. However, for 5160H and Duraspring steels, only a continuous decrease of the value with increasing hardness has been observed.

The Bauschinger stress parameter at 1pct pre-plastic strain was plotted against the Si content for all three steels hardened to HRc 48 above, and results are shown in Fig 3.11. The correlation between the Bauschinger stress parameter and Si content is very interesting indeed. The Bauschinger effect increases with the total weight percent of one third of silicon and carbon in a steel. This indicated that silicon and carbon together in a steel could have a significant influence on the Bauschinger effect, therefore, the sag resistance for the spring steel. In order to have the same value of Bauschinger stress parameter, both carbon and silicon content are exchangeable. Reducing one part of carbon means that raising three parts of silicon is needed or vice versa. Although the ductility of a material could be benefited from reducing the carbon content, further decreasing the carbon content will reduce the strength of a material because it is the carbon content that determines the hardness of martensite, therefore, the strength of a material. By contrast, increasing carbon content could increase the strength of a material with the result of sacrificing the ductility as well as toughness of a material. Nevertheless, there is no much scope for variation of the carbon content. On the other hand, Silicon content can be varied in a relatively wider range than carbon content with a maximum value of 2.2%wt in a steel.

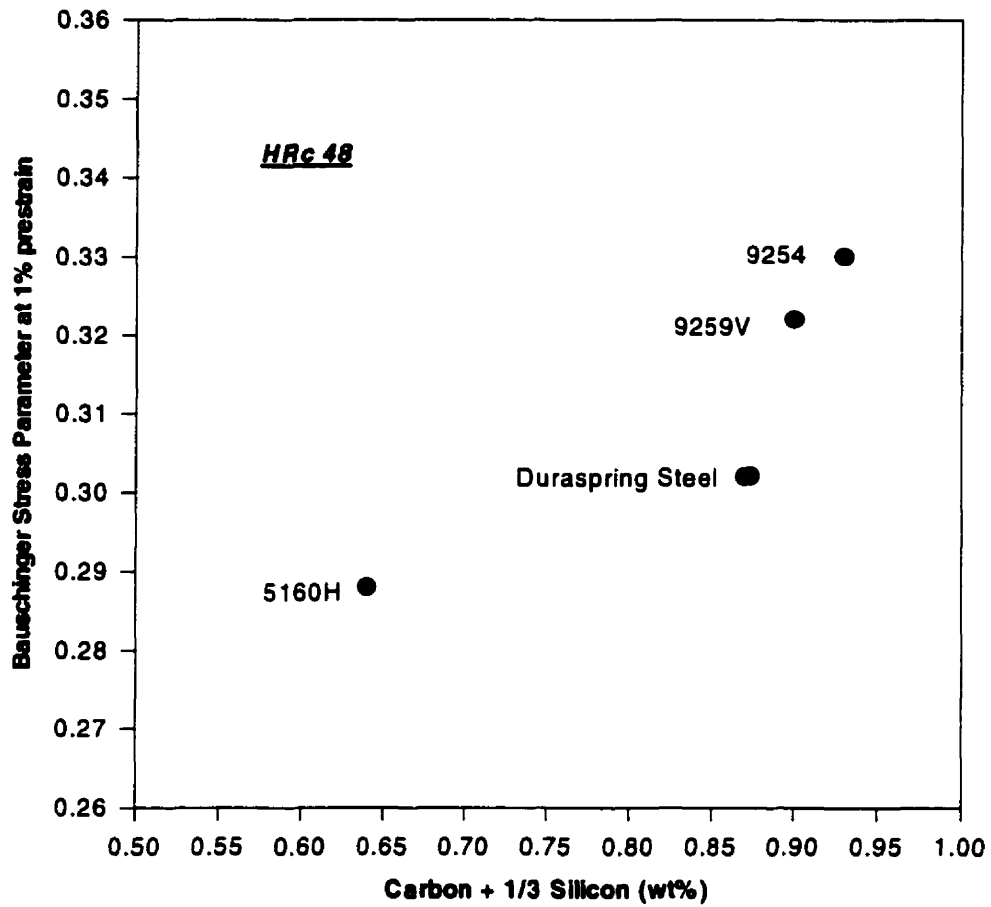


Fig 3.11 Bauschinger stress parameter at 1% pre-strain vs carbon and 1/3 silicon content when tempering to HRC 48 for 160H, 9259V, and Duraspring steels.

3.5 Examination of silicon and inclusions in spring steels

Previous results have shown that silicon concentration has a significant effect on the microstructures of spring steels after quenching and tempering by mainly influencing the carbide morphology. This effect transferably affects the mechanical properties of these spring steels, such as the hardness and the Bauschinger behavior. In a view of above, a further investigation on silicon becomes necessary, more importantly on the silicon distribution. Fig 3.12 shows the result of x-ray mapping analysis on 9259V steel from SEM.

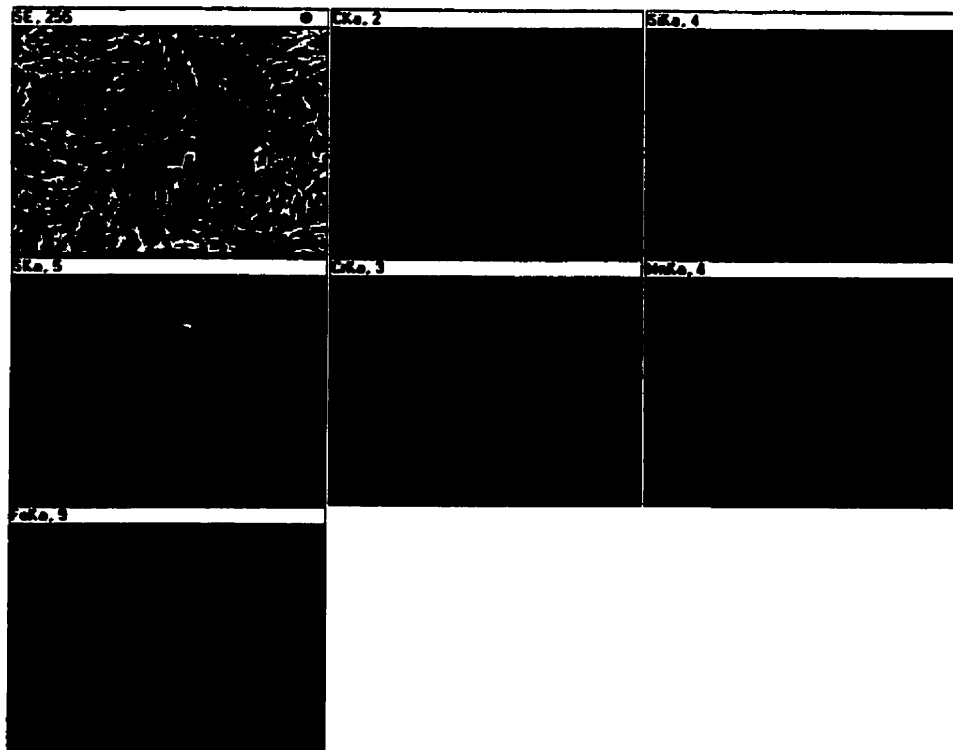


Fig. 3.12. X-ray mapping analysis of silicon and image of MnS inclusion in 9259V.

It is now generally recognized that the deformability of inclusions is a crucial factor that plays a major role not only in service where risk of fracture exists but also during hot and cold working operations. The interesting question raised drove us make the effort to detect the effect of silicon on the formation, the types, and distribution of inclusions by using Field-Emission SEM. Results are summarized as following:

- (1) In this part of the investigation, 9259V steel samples tempered to HRc 45 and HRc 50 were examined under the SEM and it has been found that globular MnS inclusions are present in the steel. The size of such inclusions ranges from 1 to 3 μm . This type of inclusion has been deformed to ellipsoidal shapes, i.e. "cigar shaped".
- (2) The X-ray mapping analysis has revealed no silicon content inside these inclusions; only occasionally, silicon was detected in association with the edges of such inclusions. This observation, therefore, confirmed that the silicon addition does not affect the formation of the conventional inclusions; Rather than this, it influences the morphology of tempered carbides.
- (3) The X-ray mapping analysis has also showed that silicon does not remain in the ultimate carbide phase to any measurable extent. In other words, silicon is nearly insoluble in the carbides. Since the maximum solution of Si in the α -Fe (ferrite) is 15-18 %, Si would be expected to distribute mainly in the ferrite matrix instead of carbides, therefore, it can have a very significant effect on the growth of precipitated carbides.

Chapter 4

4.1 Effect of silicon on tempering behavior of spring steels

4.1.1 Effect on hardness

Fig 3.1 showed that the general trend is an overall softening as the tempering temperature raised. In fully hardened martensite steels, carbon is almost entirely supersaturated in the solid solution in a body - centered tetragonal lattice and internal stresses are high, see Fig. 4.1.

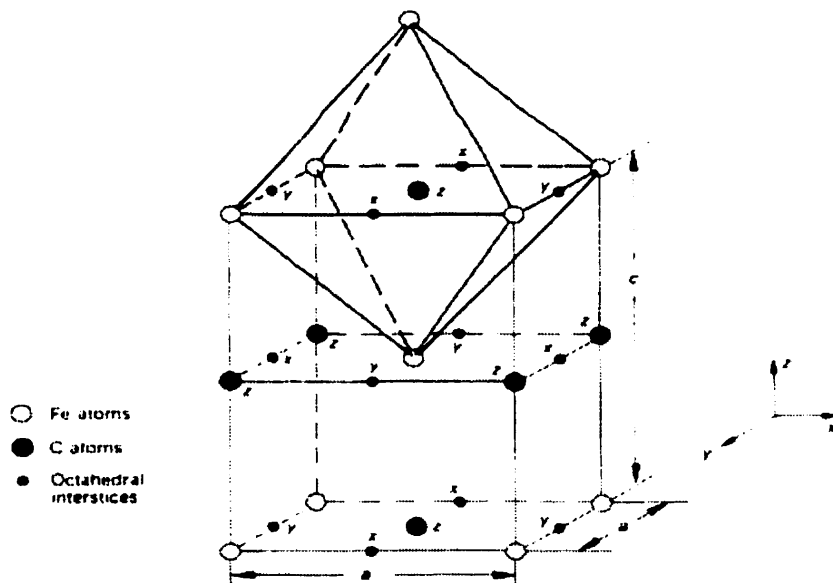


Fig. 4.1 Martensite body – centered tetragonal lattice illustrating the three sets of octahedral interstices. The z – set is fully occupied by carbon atoms^[4.1].

On tempering, carbides (ϵ -carbide) are precipitated through carbon atom diffusion out of martensite and iron atoms of the lattice are rearranged, thus providing considerable stress relief. Carbides precipitated from martensite at early stage subsequently decompose to cementite at higher temperatures. It is accompanied by a softening process due to the simultaneous removal of carbon from the martensite matrix. However, marked softening occurs at higher tempering temperatures that are mainly due to the formation of cementite and complete carbon depletion of the martensite. Of course, the formation of cementite carbide involves the diffusion of carbon atoms. Unlike substitutional solid solution, atoms move as a result of jumping into vacancies, diffusion of carbon atoms occur by jumping from one interstitial site into a neighbouring one. An expression can be written for interstitial diffusivity:

$$D = \alpha a^2 p v e^{-\Delta G_m / RT} \quad (4.1)$$

Where α is a geometrical factor that depends upon the crystal, a is the lattice parameter of the crystal, p is the number of nearest interstitial sites, v is the vibration frequency of a solute atom in an interstitial site, ΔG_m is the free energy per mole needed for solute atom to jump between interstitial sites, T is the absolute temperature in degrees Kelvin, and R is the Gas constant. Therefore, it can be seen that the diffusivity or diffusion coefficient is a function of temperature. The higher the temperature, the larger the value of D . During tempering, the diffusion coefficient of carbon increases with increasing tempering temperature, therefore, it is easier for carbon atoms to diffuse into a body-centered cubic crystal containing interstitial sites right after they are rejected from martensite, see Fig. 4.2.

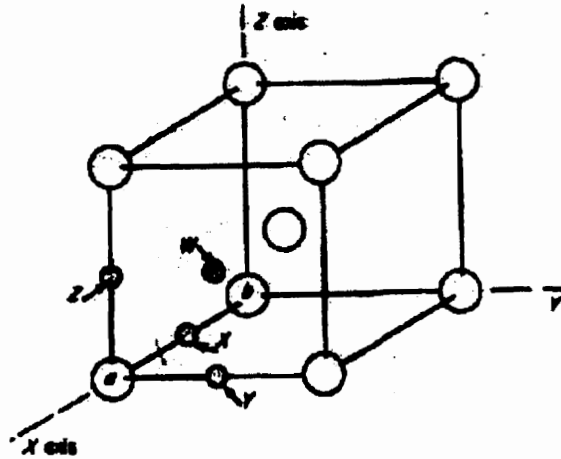


Fig. 4.2 The nature of the sites that interstitial carbon atoms occupy in the body – centered cubic iron lattice^[4.2].

This led to the formation of carbide and the growth of carbide. When a body-centered cubic crystal containing interstitial atoms, like carbon atoms, is in an unstressed state ^[4.2]. That is why a general trend of softening with increasing in tempering temperature is displayed for these three steels.

Although all three steels showed the similar tempering behavior, the 9259V demonstrated the highest hardness at all temperatures tested mainly because of its highest carbon content and its relatively high silicon content among the three steels. It is interesting that again the Duraspring steel, despite its lower carbon content, always has higher hardness than 5160H. The above results indicate clearly that the hardness of tempered martensite is no longer influenced solely by carbon content. In fact, the effect of carbon on hardness decreases markedly with increasing tempering temperature as carbon is gradually rejected from martensite. The effect of alloying elements on hardness, therefore, could be encountered, see Fig. 4.3. and Fig. 4.4.

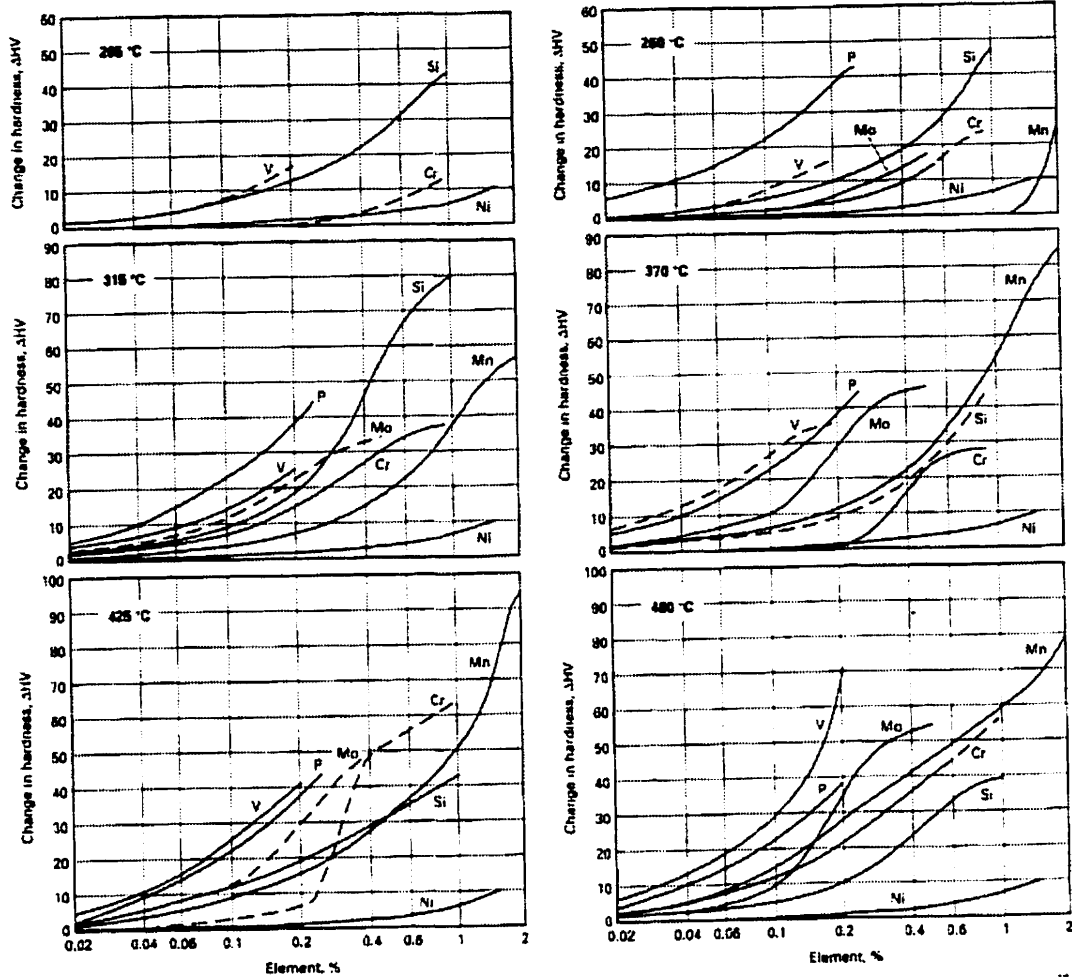


Fig. 4.3 Effect of several elements on the hardness of martensite tempered in temperature range from 205 °C to 705 °C for 1h^[4.3].

The main purpose of adding alloying elements to steel is to move the TTC curve to the right, therefore, to increase the hardenability (the capability of the steel to form martensite upon quenching from above its critical temperature). The general effect of alloying elements on tempering is a retardation of the rate of softening, especially at the higher tempering temperatures. Thus to reach a given hardness in a given period, alloy steels require higher tempering temperatures than carbon steels do.

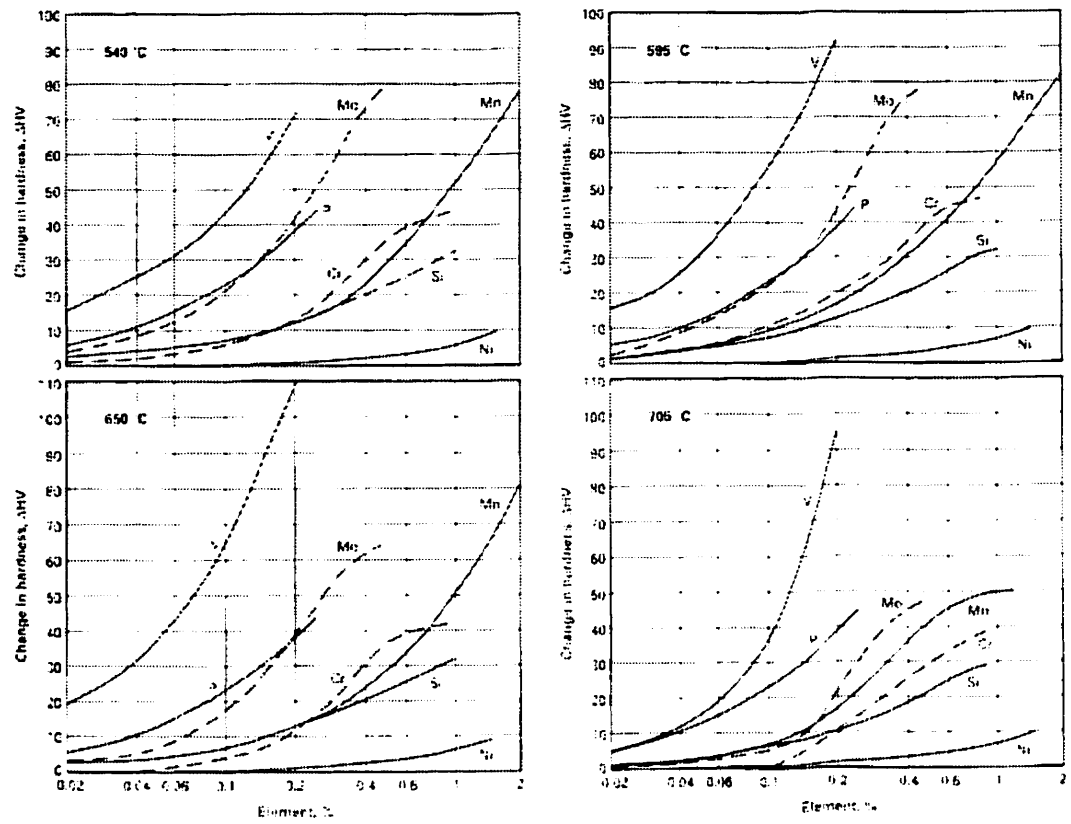


Fig. 4.4 Effect of several elements on the hardness of martensite tempered in temperature range from 205 °C to 705 °C for 1h^[4.3].

In this case, silicon addition in the Duraspring steel (0.47% C, 1.22% Si) increased the hardness at all tempering conditions compared to 5160H (0.55% C, 0.28% Si). The effect of silicon on tempering of spring steels has been studied for many years. It has been well known that the presence of higher silicon content in steel can inhibit the conversion of ϵ -carbide to cementite or the growth of the carbide, therefore, retarding the softening^[4.4]. Actually, it is the size, shape, composition, and distribution of the carbides formed during tempering that primarily determines the hardness and other properties along with a relatively minor contribution from solid – solution hardening of the ferrite^[4.3].

Why does silicon addition have such an effect on the growth of carbide? The silicon atom has a similar atomic radius compared to the iron atom. With silicon present in steel, it forms substitutional solid solution in α -Fe (ferrite). The maximum solubility of silicon in ferrite is about 15% at room temperature. Thus, with the quantity of silicon present in Duraspring steel (1.22%Si), it should be completely soluble in iron even with the presence of other alloy elements. It is not likely that silicon presents in any large proportion in the carbide. An alloying element having a higher solubility in the carbide than in ferrite is not likely to have a large effect on the growth of the carbide, although it may control the structure of the carbide precipitated, the nucleation sites, and the rate of nucleation. If the alloying element is nearly insoluble in the carbide, it can have a very large effect on the rate of growth of precipitated carbides ^[4.5]. Owen ^[4.6] explained this as being caused by a necessity for Si to diffuse away from a growing carbide particle. As Si is rejected from the carbide, its concentration in the surrounding matrix rises. Because Si increases the activity of C in ferrite, or decreases the activity of C in martensite, the gradient in C activity causing the C atoms to diffuse toward the growing carbide particle is decreased by the accumulations of Si. Therefore, the growth of carbide is retarded. A sufficient amount of energy is needed for silicon to diffuse away so that the carbide could grow up. This means a higher tempering temperature is necessary to provide sufficient energy, see Fig 4.3. In addition, silicon produces solid solution hardening of ferrite matrix. Both effects contribute to the difference in hardness between low silicon steel (5160H) and high silicon steel (Duraspring steel). Actually, the effect of silicon on the hardness becomes more apparent at around 300 °C tempering temperature.

From Fig 3.1, it also can be noticed that the rates of reduction in hardness are different among these three steels in different temperature ranges. At low tempering temperature range (250 - 350 °C), the rate of reduction is smaller. At higher tempering temperature range (above 400 °C), the rate of reduction in hardness is larger. Since the diffusion of carbon in the martensite is a rate-controlling process, it is likely that silicon addition reduces the carbon-activity involved in the precipitation of ϵ -carbide, hence, the rate of precipitation decreases. The decrease is so profound with higher silicon content that the separation between the first stage and third stage of tempering is more definite than in the low silicon steel because the epsilon carbide is stabilized and the subsequent precipitation of cementite is retarded. This situation results a relative plateau in the curve (Fig. 3.1) at temperature between 250 and 400 °C for Duraspring steel, a smallest rate of reduction in hardness among the three. In the low-silicon steels, the third stage can be split into two processes. Process one, cementite of the thin-plate type precipitates from the low-carbon martensite remaining after the first stage, but the epsilon carbide does not precipitate in the reaction to any substantial degree, it persists while the cementite is forming. Process two, at a later time or higher temperature, the epsilon carbide dissolves or decomposes to produce more cementite when the matrix is suitably drained of carbon. This causes further softening. With the presence of higher silicon contents, it retards the precipitation of cementite sufficiently so that the two processes merge into one and onset of third stage is delayed to a higher temperature range where epsilon carbide can readily dissolve or decompose ^[4.7]. The rate of reduction becomes greater after tempering at above 400 °C. This indicates that the effect of silicon in inhibiting the conversion of epsilon carbide to cementite or the growth of carbides is no longer sufficient enough to permit tempering at higher temperature with less

loss of hardness, see Fig. 4.3, even with the effect of silicon on solid solution hardening of ferrite matrix. Subsequent changes of cementite morphology along with recrystallization of ferrite cause further softening.

4.1.2 Effect on microstructure

The optical metallographic examinations of the three steels under all tempering conditions were carried out. The microstructures of the three steels are similar and are all composed of tempered martensite, carbides, and ferrite matrix. The average length of martensite lath is longer in 5160H, but is smaller in both Duraspring and 9259V steels. As the size of martensite largely depends on the austenite grain size, the above observation indicates that the Duraspring steel and 9259V have smaller grain size. Alloy elements such as V, Si and Mn in these steels are assumed to be responsible for the differences.

More importantly, there are significant differences in the carbide morphology among these three steels, see Fig. 3.4 to Fig. 3.7. The carbides in 9259V and Duraspring steels are spherical, small, and closely spaced, whereas the carbides in 5160H are rod-shaped, larger, and more widely spaced. Clearly, the differences in characteristics of the carbides are associated with the difference of silicon concentration among these steels. The present observation has confirmed the results by Tata and Driscoll^[4,8]. It has been suggested that the silicon addition present in the steel can reduce the growth rate of carbide precipitates, therefore, the rate of coarsening of carbides. The coarsening of carbides in the steel is an important phenomenon that influences markedly the mechanical properties. The driving force for coarsening of the carbide is provided by the reduction of surface energy of the carbide. In order for the ϵ -carbide to cementite transition and for the cementite coarsening reaction to proceed, a net migration of iron atoms from the growing particles to the dissolving particles

is necessary, leaving a higher density of vacancy at the growing particles ^[4.9]. When silicon addition is present, the activity of carbon in particles is apparently reduced. This leads to a reduced particle coarsening rate. In short, high silicon content stabilizes the ϵ -carbide formed during the first stage of tempering, inhibits the growth of cementite, suppresses the third stage of tempering, and therefore, refines the carbides. It will be soon shown in the subsequent section that the difference in characteristics of carbide caused by the silicon content has the major influence on the difference of Bauschinger effect, thereby, the relaxation or sag characteristics of the spring steels.

4.2 The Bauschinger Effect

4.2.1 Bauschinger effect vs. pre-plastic strain

Experimental work conducted on 5160H, 9259V, and Duraspring steels were designed to explore the manifestation of the Bauschinger effect under different pre-plastic strain levels and different hardness levels. It has been mentioned in the introduction section that the Bauschinger effect is an indirect measurement of sag behavior because sag is the phenomenon that cyclic microcreep occurs over a large number of loading cycles at stress levels clearly below the material's yield strength and the Bauschinger effect is the phenomenon which occurs only at the first few cycles of loading, hence, the mechanisms of the Bauschinger effect are not responsible for sag behavior. However, Furr ^[4.10] showed in his work on many different kinds of materials that a qualitative relationship exists between sag resistance in springs and the size of the hysteresis loops generated in the torsional Bauschinger test. A similar relationship was confirmed by Brownrigg and Sritharan ^[4.11] in tension and compression tests. That is the higher the Bauschinger effect, the better the sag

resistance of the spring steels. The present investigation was done by measuring the effect in tension and compression rather than torsion. It does not invalidate the applicability of the test to springs because the basic mechanism of plastic deformation in both loading modes is dislocation motion. The hysteresis loop data in tension and compression can easily be expressed in stress-strain terms independent of the test piece dimensions. The original Bauschinger effect was described as a yield-lowering effect. To quantify the change in the flow stress upon stress reversal, a number of different parameters termed Bauschinger effect parameter have been employed. These parameters reflect the mechanisms involved in lowering the yield stress. One of these parameters, Bauschinger stress parameter, is used to compare the internal stresses developed during the forward deformation. The Bauschinger stress parameter is the fraction of the total work hardening arising from the back stress and has the form $\beta_{\sigma} = \sigma_b / 2\sigma_f = (\sigma_f - \sigma_r) / 2\sigma_f$. Where σ_b is the back stress, σ_f is the forward flow stress, and σ_r is the yield stress upon reloading in the opposite direction. The smaller the value of β_{σ} , the smaller the Bauschinger effect. In the present study, Bauschinger stress parameter was used as the measure of Bauschinger effect because the ideas of internal back stresses were believed to be the main cause of the Bauschinger effect here. The detailed consideration in this concept was given by Masing on Brass^[4,12]. In the forward and reversed deformation, dislocations would interact with each other or with second phase particles that may make many of the original mobile dislocations immobile. With the increase of pre-plastic strain, the number of dislocations generated increases. Since the magnitude of back stress largely depends on the number of dislocation pileups and mobile dislocations available in the dislocations pileups, the increased number of dislocations can be utilized to produce higher back stresses. Consequently, the higher the pre-plastic strain, the larger the

Bauschinger effect. However, further increasing the pre-plastic strain would not only increase dislocation density but also increase the chance of dislocation interactions. Consequently, some dislocations can interact with each other to produce jogs that may lock each other. Thus they may fully or partially lose their mobility. Eventually, a constant ratio of mobile to immobile dislocations in the material can be reached. Hence, it is expected that a saturation of back stress in the material can be reached, and so the Bauschinger effect reach a saturation value at a certain pre-plastic strain level.

One thing that should be noted is that there are many factors that would affect the value of Bauschinger effect. Among these factors, there are grain size, chemical composition, distribution of precipitated particles, pre-strain levels, hardness, temperature, strain rate. In the present study, the effects of grain size, temperature and strain rate were beyond the scope and they were kept as a constant. Fig. 3.9 showed the results of Bauschinger stress parameter against plastic pre-strain. The Bauschinger effect increases with increasing pre-strain, regardless of chemical composition, precipitate size, distribution, and hardness level of these steels, until saturation is reached at certain pre-strain level.

The low silicon 5160H steel showed a smaller Bauschinger effect compared with the high silicon Duraspring spring steel while 9259V steel demonstrated the highest Bauschinger effect at all plastic pre-strain after they have been hardened to HRc 47 and above. Based on the previous and present studies, the effect of silicon addition on the tempering of spring steels is demonstrated in the notable change in the carbide morphology formed during tempering. This difference in carbide characteristics is responsible for the difference in Bauschinger behavior of these steels. Apparently, smaller, more numerous, spheroidal, and closer spaced carbides in both 9259V and Duraspring steels have provided more effective

barriers to dislocation motion and promoted the formation of more dislocation pileups. This, therefore, can produce higher back stresses during forward plastic deformation. The effect of solid solution hardening from silicon and other alloy elements is also responsible for the dislocation motion and pileups because they can raise the strength of the ferrite matrix in which the carbides are imbedded. The strong ferrite matrix may have a strong interface between carbides and ferrite matrix, and therefore, it can hold more dislocations in each dislocation pileup. All the factors discussed above will give the high silicon steels higher stresses when deformed to the same strain level; consequently, a larger Bauschinger effect should be exhibited.

The above discussion answered the question why the high silicon steels demonstrate higher Bauschinger effect than low silicon steels. Still another question could be raised, that is why 9259V has a stronger Bauschinger effect than Duraspring steel regardless of even higher silicon content in the Duraspring steel? In order to answer this question, it is necessary to take a closer look at major alloying elements of these two steels again. Duraspring steel has higher silicon and manganese content but a lower carbon content compared to 9259V. This indicates that both carbon and silicon have strong influences on the Bauschinger effect. The number of carbide precipitates during tempering mainly depends on the carbon concentration. Generally speaking, the higher the carbon content in the steel, the greater number of carbides that would precipitate in the steel during tempering. With the help of alloy elements, such as silicon, carbides formed during tempering get refined. This kind of larger number, more closely spaced, and further refined carbides would enhance dislocation pileups, therefore, increase the back stress which is responsible for the Bauschinger effect. In addition, these closely spaced carbides may significantly increase the number of dislocation

pileups, therefore, can produce higher overall back stress when the same level of plastic strain is applied. As the result, the 9259V showed a higher Bauschinger effect than the Duraspring steel at all pre-plastic strain levels.

4.2.2 Bauschinger effect Vs hardness

As being well accepted, the higher the Bauschinger effect, the better the sag resistance of the spring steels ^[4.13]. The question of interest now becomes how the hardness affects the Bauschinger effect, therefore, the sag behavior of the spring steels. This is especially important at higher hardness levels at which the weight reduction of springs could be realized. Fig 3.10 shows the value of Bauschinger stress parameter against hardness at 1 % pre-plastic strain level. A maximum value of Bauschinger effect at around HRc 50 with 9259V is observed, and a continuous decrease of Bauschinger effect is displayed for both 5160H and Duraspring steels. These results come to a good agreement with M.Assefopor-Dezfuly and Brownring's work ^[4.14] on a number of microalloyed and standard grade spring steels. As we have known, the cause of the Bauschinger effect is the back stress that can assist the motion of dislocations in the reverse direction. The dislocation pileups at grain boundaries and Orowan loops around carbides are the two main sources of the back stress. On tempering, the ferrite matrix is usually strengthened by grain refinement as tiny carbide particles will impede grain growth. It will also be strengthened by solid solution mechanisms of alloy elements, such as Si. Furthermore, the carbide morphology itself formed during tempering is also affected by alloy addition. Fig. 3.10 shows an increase in the Bauschinger effect for both 9259V and Duraspring steels as hardness decreases from HRc 54 to Hrc 50. As tempering temperature is raised, the dislocation density decreases, ϵ -carbides formed

during the first stage of tempering tend to transform to cementites, and at the same time new carbides would keep forming. Because of higher silicon content in both 9259V and Duraspring steels, the carbide particles are numerous, small, closely spaced, and mostly distributed along grain boundaries. When such a structure is subjected to a plastic deformation, these carbides would provide sufficient sites for dislocation pileups. This results in an increase in back stress over this hardness range. If a higher tempering temperature is employed, hardness will further decrease as cementite particles coarsen and become spheroidized. Also happened are the recrystallization of ferrite, the further rejection of carbon from martensite, and the further loss of the trigonality of martensite. For the 9259V steel, a finer, smaller, and closely spaced carbide morphology can be observed. It certainly can introduce more effective barriers to the dislocation movement. Although more sites are available for dislocation pileups as the carbide particles become denser, i.e. dislocations can be also pinned by these numerous and small carbides, therefore, either partially or fully lose their mobility. Once the dislocations lose their mobility, they would no longer contribute to the back stress as well as the Bauschinger effect. That is the reason a decrease of the Bauschinger effect is displayed for 9259V steel as the hardness decreases or the tempering temperature increases. From a different perspective, the above results indicate that the magnitude of back stress depends not only on the number of sites available for the dislocation pileups but also on the number of mobile dislocations in each pileup. The former can be determined by the number of carbides and their morphology, more precisely, the carbon and silicon contents in the steel. The latter would be associated with the dislocation density and the dislocation interaction, which very much depend on the tempering temperature applied.

Both 5160H and Duraspring steels showed continuous increase of the Bauschinger effect while the hardness further decreases or the tempering temperature further increases. For Duraspring steel, because of its higher silicon content, the conversion of ϵ -carbide to cementite is inhibited and the growth of carbide is also retarded. In other words, it permits a higher tempering temperature without losing the stability of carbide. This would remain the finer carbide morphology even at a higher tempering temperature, therefore, still can provide sufficient sites for the dislocation pileups. On the other hand, as the tempering temperature increases, the dislocations become less dense and the chance for dislocation interaction is reduced. This would increase the mobile dislocations in the pileup. All of the above, a higher back stress can be expected when this kind of structure is subjected to a plastic deformation, therefore, a higher Bauschinger effect can be exhibited. For 5160H, a slight increase of the Bauschinger effect is displayed as the temperature increases. As we have known, its carbides are larger, rod-shaped, and widely spaced because of its lower silicon content, therefore, short-range effects, such as the annihilation of the mobile dislocations during reverse straining are weak. However, as increasing tempering temperature, the long-range internal stresses that assist the motion of dislocations in the reverse direction become stronger because of the pile-up of dislocations and Orowan loops around strong precipitates. This could be due to the secondary hardening by chromium. Chromium is a strong carbide forming element. It does not form chromium carbide at lower tempering temperatures because of the fact that at lower temperatures the rate of diffusion of this substitutional element is too slow to permit its formation. Cementite can form because the diffusion rate of carbon is still very large. However, when the tempering temperature is high enough, appreciable amount of chromium carbides would be precipitated and they are stronger than cementite. This kind of

strong particle certainly has a better coherency with matrix and a strong interaction with dislocations, thus, produces higher internal back stresses which result a strong Bauschinger effect.

In summary, the magnitude of the Bauschinger effect of 5160H and Duraspring steels showed a continuous decreases with increase of hardness, whereas a maximum value of the Bauschinger effect at around HRc 50 can be detected for 9259V. Carbide morphology formed during tempering and different hardening mechanisms associated with certain tempering stages are responsible for these different behaviors. The present results again show that the silicon and carbon contents have a major influence on the carbide morphology, and therefore, the Bauschinger behavior of the spring steels. From Fig 3.10, 9259V demonstrated the strongest Bauschinger effect among the three steels. Thus, it should be expected that 9259V have a better sag resistance than the other two. Duraspring steel is also expected to have a better sag resistance than 5160H.

4.3 Estimation for weight saving

In the earlier section, we have already discussed the new trend of making lighter vehicles. Automotive suspension springs are no exception to the weight reduction. To cut the weight of suspension springs, the sag resistance should be improved because the operating stress is likely a higher fraction of the yield stress of the material. The simplest way to do this is to raise the hardness of the spring steels. From the previous section, the results showed that the 9259V have a larger Bauschinger effect or a better sag resistance after its hardness is raised from HRc45 to HRc 50. Then such a high performance should be realized on the design of springs as for weight saving.

For this purpose, the following calculations could be considered.

Table 4.1 Assumptions

| FACTORS | | NORMAL | WEIGHT SAVED |
|--------------------|----------|--------|-----------------|
| Wire dia. mm | variable | d | d _s |
| Mean coil dia. mm | constant | D | |
| Spring height mm | constant | H | |
| Active coils | constant | N | |
| Spring rate kgf/mm | constant | K | |
| Weight kgw | obtained | W | W _s |

Table 4.2 Calculations

| NOMAL | WEIGHT SAVED |
|-------------------------------------------------------------------------------------------------------------------------------|---------------------------------------------------------------------------------------------------------------|
| Torsion stress : τ $\tau_o = 8 \times D \times P / \pi \times d^3$ | $\tau_{os} = a \times 8 \times D \times P / \pi \times d_s^3$ a : increasing factor P: applied load |
| SPRING RATE : K $K = G \times d^4 / 8 \times N \times D^3$ G : the modulus of rigidity (8000 kgf/mm ²) | |
| Weight saving rate : ΔW $\Delta W = \{ (W - W_s) / W \} \times 100\%$ | |

From the equations above,

$$d = (8 \times D \times P / \pi \times \tau)^{1/3} = A (\tau)^{1/3} \quad (4.2)$$

$$W = V \times G = N \times \pi \times D \times (\pi \times d^2 / 4) \times G = B \times d^2 \quad (4.3)$$

$$\Delta W = \{ (W - W_s) / W \} \times 100\% = 1 - (\tau_s / \tau)^{-1/3} \quad (4.4)$$

When the hardness is raised from HRc45 to HRc 50, the yield strength can be raised from 1400 MPa to 1688 MPa. The yield strength increased 20 %. The reduction in weight is 12 %. This means that when it is available to increase the strength of the material 20 %, it becomes possible to produce suspension springs that have the same performance (i.e. main coil dia., spring height, spring rate, etc.) but are 12 % lighter. Speaking of spring design, however, it is necessary to consider the effects of the shape of the spring tail end and spring sheet. More importantly, the performance of materials that are made of the springs, such as sag resistance, fatigue properties, has to be taken into consideration.

4.4 Reference

- 4.1 S. R. Honeycombe, and H. K. D. H. Bhadeshia, *STEELS – microstructure and properties*, second edition, 1995, pp88
- 4.2 R. E. Reed-Hill, *Physical Metallurgy Principles*, third edition, Boston, 1994, pp.405.
- 4.3 *Heat Treating*, ASTM handbook, vol. 4, 1991, pp.128.
- 4.4 E. C. Bain, *Steel*, American Society for Metals, Metals Park, Ohio, 1939, pp.239.
- 4.5 W. C. Leslie, and G. C. Rauch, *Met, A*, 9A, 1978, pp. 343.
- 4.6 W. S. Owen, *Trans. Am. Soc. Met.*, vol. 46, 1954, pp.812.
- 4.7 C. J. Altstetter, Morris Cohen, and B. L. Averbach, *Effect of Silicon on the Tempering of AISI 43XX Steels*, *Trans*, vol 55, 1962, pp.287.
- 4.8 H. J. Tata, E. R. Driscoll, and J. J. Kary, “Steels for automotive coil springs with improved resistance to relaxation”, *SAE Technical Paper Series 800480*, Feb 1980.
- 4.9 R. M. Hobbs, G. W. Lorimer, and N. Ridley, “Effect of silicon on the microstructure of quenched and tempered medium carbon steels”, *JISI*, Oct 1972, pp.757.
- 4.10 S. T. Furr, “Laboratory Studies of Low Chromium and Chromium – Free Steels for Suspension Coil Springs”, *SAE Technical Paper Series 800479*, Feb 1980.
- 4.11 A. Brownrigg, and T. Sritharan, *Mater. Rorum*, 1987, vol. 10 (1), pp. 58-63.
- 4.12 G. Masing, *ibid.*, 1926, 5, pp.135.
G. Masing, *ibid.*, 1926, 5, pp.142.
- 4.13 S. T. Furr, “Development of a New Laboratory Test Method for Spring Steels”, *Transations of the ASTM: Journal of Basic Engineering*, 94, 1972, pp. 223-227.

- 4.14 M. Assepour-Dezfuly, and A. Brownrigg, "Parameters affecting sag resistance in spring steels", *Metallurgical Transactions A*, 1989, vol. 20A, pp. 195.

Chapter 5

1. Systematic experimental work was conducted on the study of tempering behavior of the 9259V, 5160H, and Duraspring steels. A general softening trend with increasing temperature is displayed for all three steels. Both the reduction in hardness and the rate of such reduction upon tempering of all three steels are found to depend on the tempering temperature, temperature range, and alloy elements present in the steel. High silicon content again has been found to improve tempering resistance and hardness of the steels. The 9259V demonstrated the highest hardness and 5160H, on the other hand, displayed the lowest hardness under all the tempering conditions employed. Duraspring steel, even with its lowest carbon concentration among the three, showed a higher hardness than 5160H because of the effect of silicon on the hardness.
2. Optical metallographic examination again revealed that the microstructure of 9259V and Duraspring steels contain small, spheroidal-shaped, and closely spaced carbide particles, in contrast, 5160H contains larger, rod-shaped, and widely spaced carbides. The difference in carbide characteristics is attributed to the different silicon contents among the three steels. The higher the silicon content, the finer the carbides in the steel.
3. SEM X-ray mapping analysis performed on 9259V showed no evidence that silicon is present in either carbides or inclusions. Only occasionally, silicon is found in the area around the inclusions. SEM photo images also revealed that MnS inclusions showed up in the steel and are deformed into ellipsoidal shape at size around 1 –3 μm .

4. The Bauschinger effect tests were conducted to study the effect of hardness and deformation history, such as pre-plastic strain levels, on the Bauschinger behavior of spring steels. The results showed that the Bauschinger effect increases with increasing pre-plastic strain levels for the three steels investigated at all hardness levels. The 9259V demonstrated the strongest Bauschinger effect compared with 5160H and Duraspring steels, therefore, a better sag resistance can be expected. As hardness increases, the Bauschinger effect for both 5160H and Duraspring steels continuously decreases, whereas a maximum value was detected at hardness around HRc 50 for 9259V.
5. Silicon was found to be the major alloy element influencing the Bauschinger effect by the way of carbide refinement and solid solution hardening of ferrite matrix. Therefore, it is the major element affecting the room temperature sag resistance of the spring steels.
6. When the hardness is raised along with the proper designing of the spring, a considerable weight saving becomes possible.

Future work

1. To establish a relationship between the Bauschinger effect and sag resistance in terms of energy, and therefore, a better way to characterize sag behavior of spring steels.
2. To further investigate the effect of silicon content and other alloy elements on the microstructure, tempering behavior, and carbide morphology of spring steels
3. To study the effect of microstructure on the relaxation behavior of spring steels.
4. To further investigate the effect of hardness on the Bauschinger effect for other grades of spring steel.